

ATLAS新物理和新奇特强子态的寻找

陈新

清华大学物理系



Seminar at USTC

2023/07/21

么正变换

对波函数和哈密顿算符做U(1)么正变换，发现薛定谔方程形式不变（Fock）

$$\hat{H} = \frac{1}{2m} (\hat{\mathbf{p}} - q\vec{A})^2 + q\Phi$$

$$\begin{array}{l} \psi \rightarrow \psi' = e^{i\theta} \psi \\ \hat{H} \rightarrow \hat{H}' = e^{i\theta} \hat{H} e^{-i\theta} \end{array} \quad \Rightarrow \quad \hat{H}' \psi' = i\hbar \frac{\partial}{\partial t} \psi'$$

其效果是对磁矢势做规范变换 $\vec{A} \rightarrow \vec{A} + \frac{\hbar}{q} \vec{\nabla}\theta$

根据Noether定理，每一种对称性的背后都有一个守恒量。在量子场论中，如果系统规范不变，则系统电荷守恒

规范不变性与Yang-Mills理论

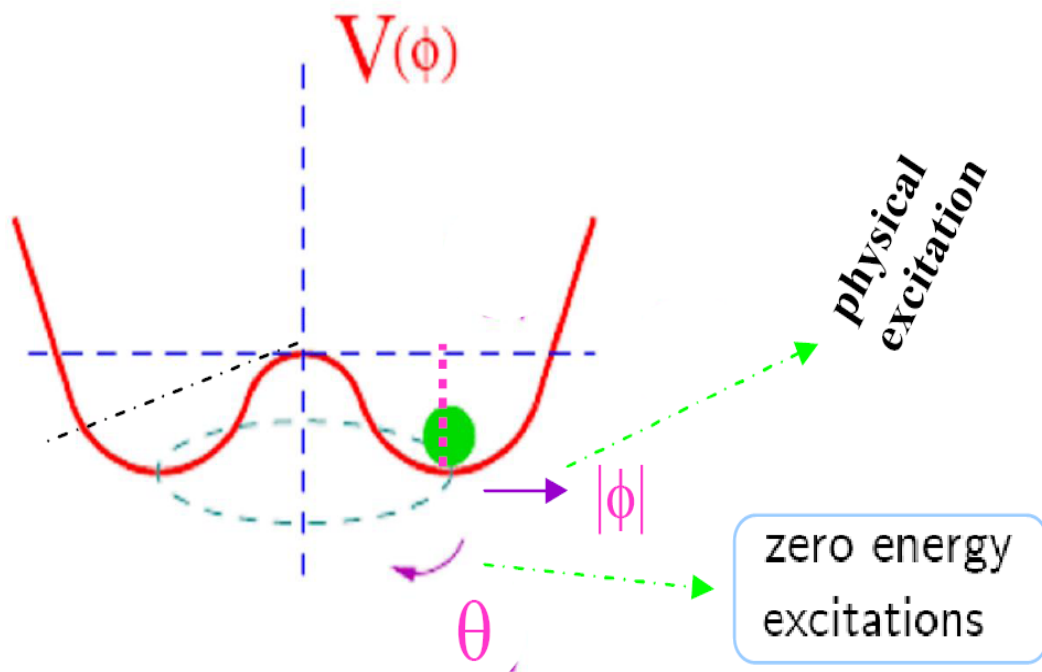
- 规范不变对系统的拉格朗日形式做出了严格的限制，基于规范不变思想的量子场论曾被Pauli提出（1953），可惜没有正式发表
- 杨、Mills二人发展了这一思想，把规范不变从电磁U(1)相互作用拓展到了SU(N)相互作用，对SU(N)相互作用的形式作出了限定。美中不足的是，规范不变性成立的前提是所有基本粒子质量为0，这显然与实验不符，这也是Pauli没有发表他早期研究的原因
- 后来希格斯等提出了基于自发性对称破缺的机制来解释为什么粒子质量不为0。2012年希格斯粒子的发现，使得基于规范不变和希格斯质量机制这两大支柱的粒子物理“**标准模型**”得以最终确立

规范不变性与Yang-Mills理论

杨振宁和米尔斯



希格斯场的势能

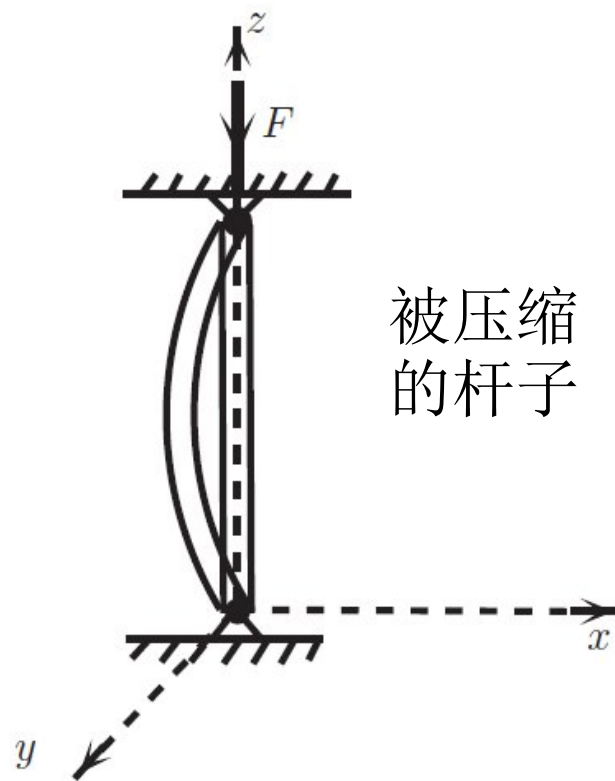
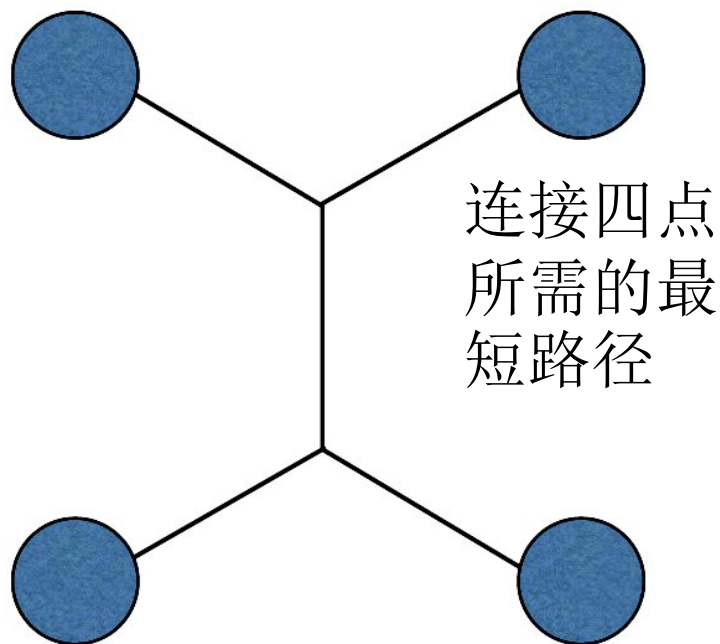


$$V = -\mu^2 \phi^+ \phi + \lambda (\phi^+ \phi)^2$$

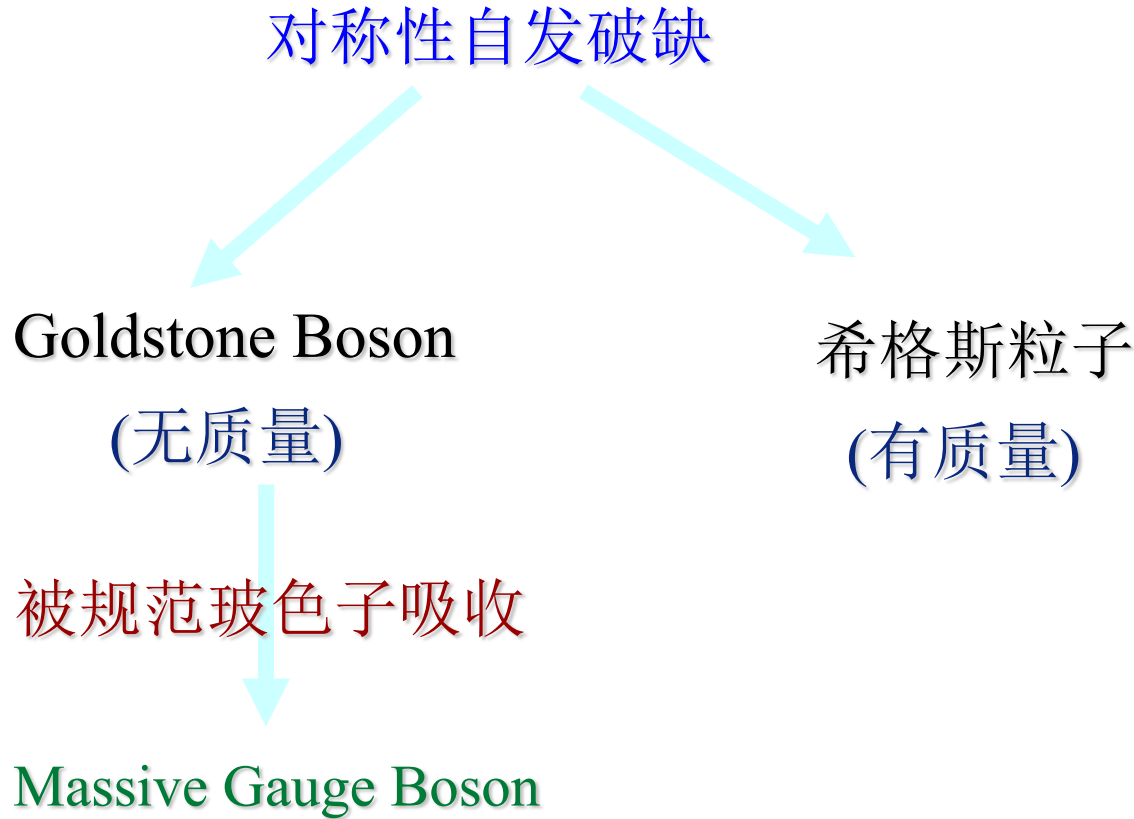
体系的基态可以是各方向简并基态的线性叠加-从而保持体系的对称性，但实际上自然的选择是其中某个方向

自发性对称破缺机制

自发性对称破缺机制：具有较高对称性系统的基态解具有较低对称性



希格斯机制



- 质量和电荷一样是粒子的一种属性

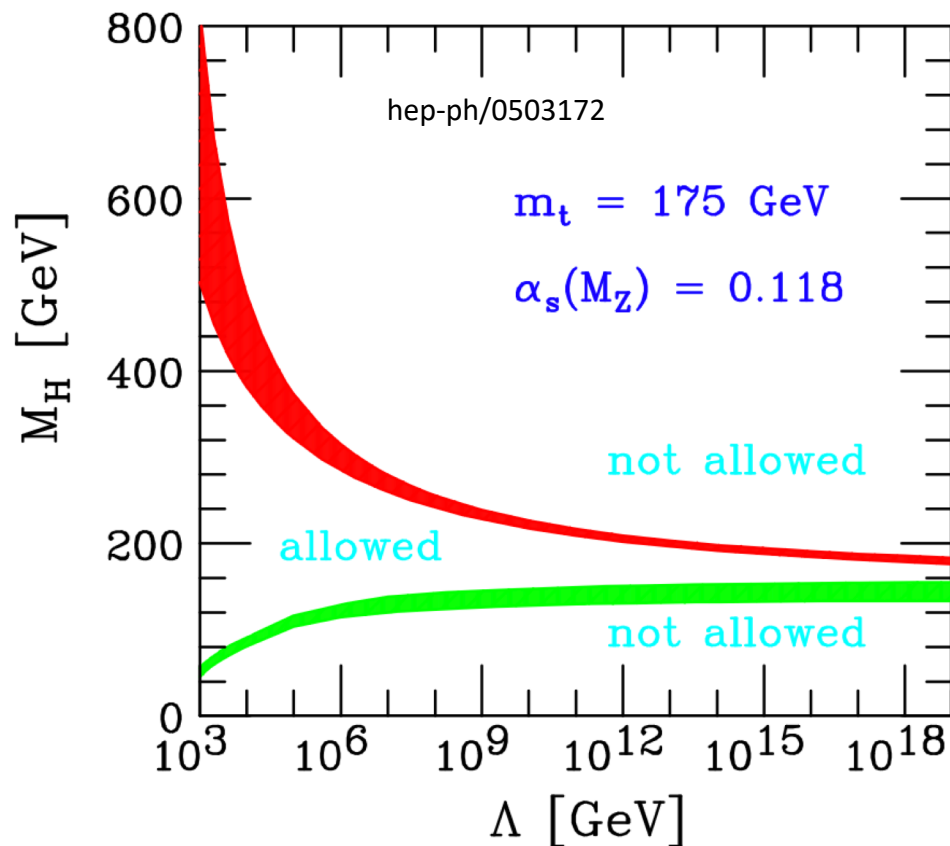
- 不同粒子质量来自于和希格斯场的相互作用

- 希格斯粒子是希格斯场的物理激发态

- 其他三个零质量激发态被规范玻色子吸收: W, Z玻色子

格德斯通玻色子被W/Z玻色子吸收后，成为W/Z纵向极化的自由度（一石二鸟）。同时，规范理论得以保持 – 希格斯机制

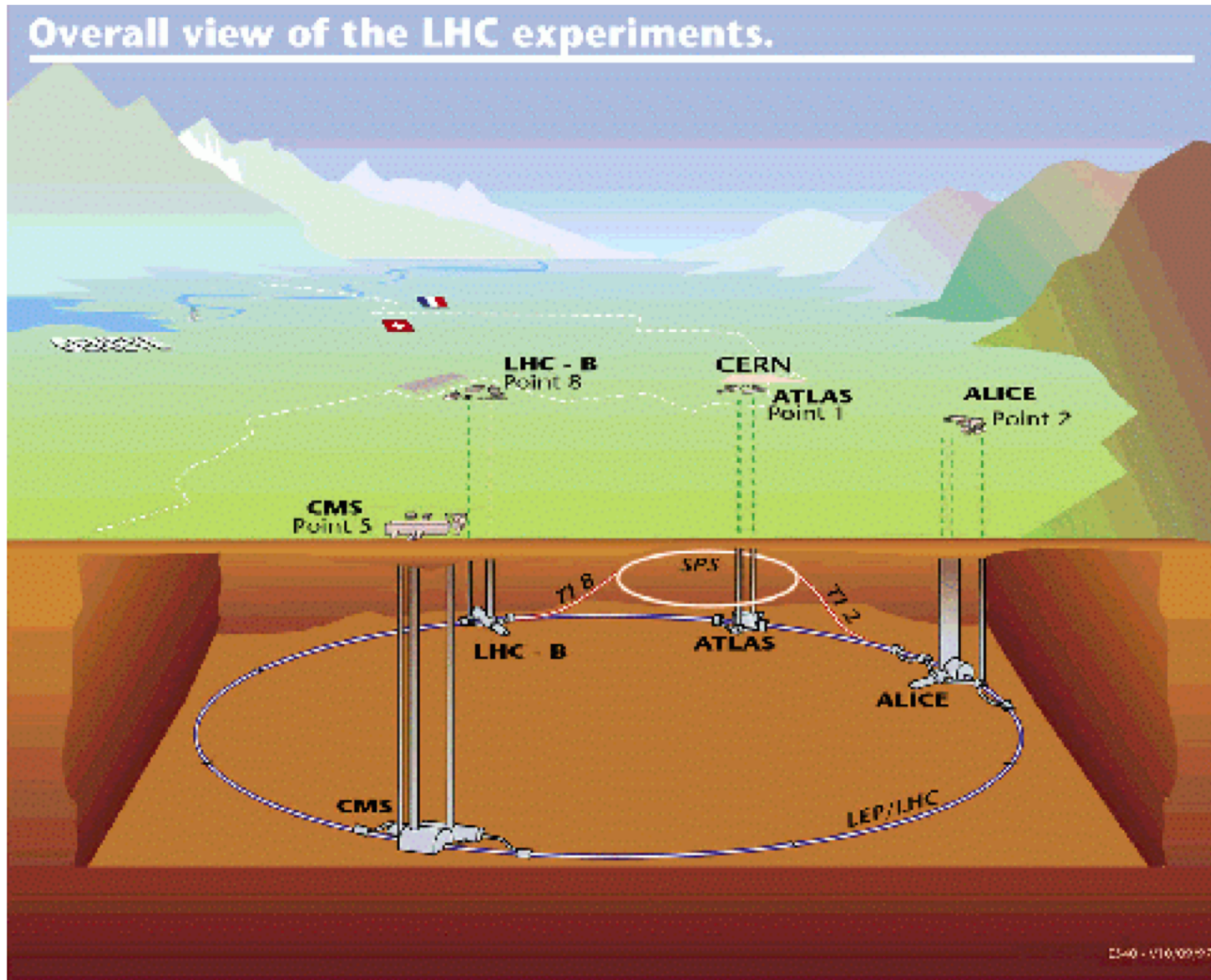
Higgs质量的理论预期



- Λ : 物理过程的能量标度，或者新物理出现的能标
- 红带子：triviality上限。Higgs自耦和系数要保持有限，Higgs粒子的质量就有一个上界
- 绿带子：真空稳定性下限。如果Higgs质量太小，则场势能没有最低点 - 真空也将不稳定

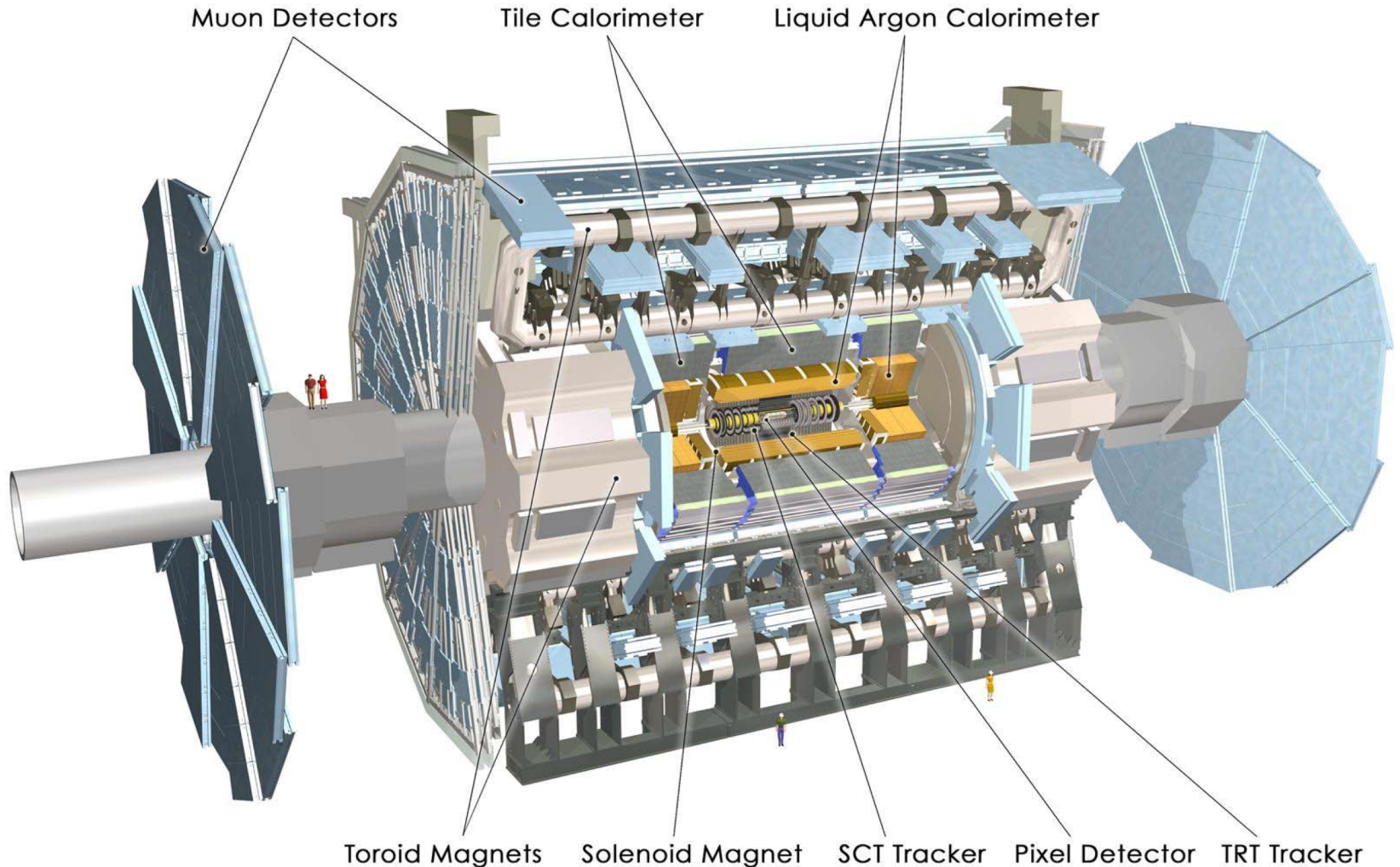
- 如果SM一直到大统一理论的能标 (10^{16} GeV) 都正确，那么希格斯粒子的质量约为 $130 \text{ GeV} \lesssim m_{\text{Higgs}} \lesssim 180 \text{ GeV}$
- 要么Higgs必然存在，要么有新物理（即超出标准模型SM的物理） - LHC

Why LHC?

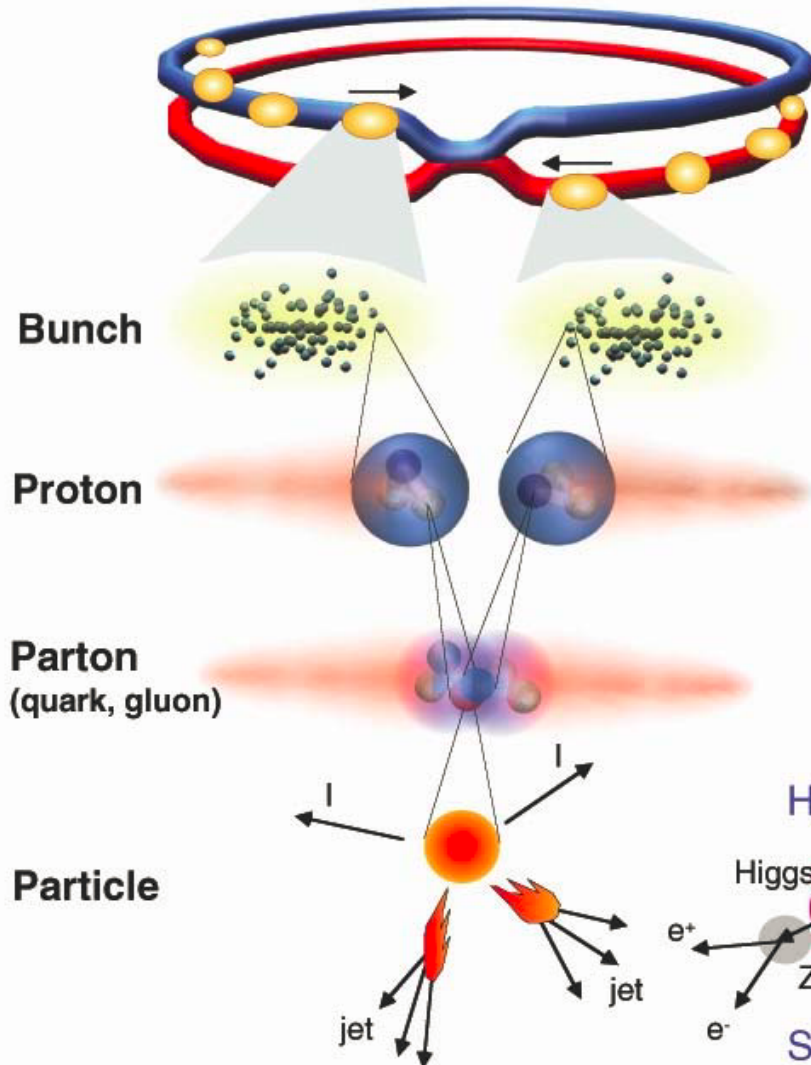


The ATLAS Detector at the LHC

Large Muon Spectrometer and SC Toroid Magnets: standalone muon momentum measurements in the muons largest air-core magnet for the first time in a collider detector



LHC: 质子-质子对撞



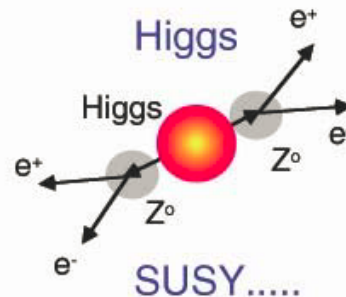
Proton-Proton	2835 bunch/beam
Protons/bunch	10^{11}
Beam energy	7 TeV (7×10^{12} eV)
Luminosity	$10^{34} \text{ cm}^{-2} \text{ s}^{-1}$

Crossing rate 40 MHz

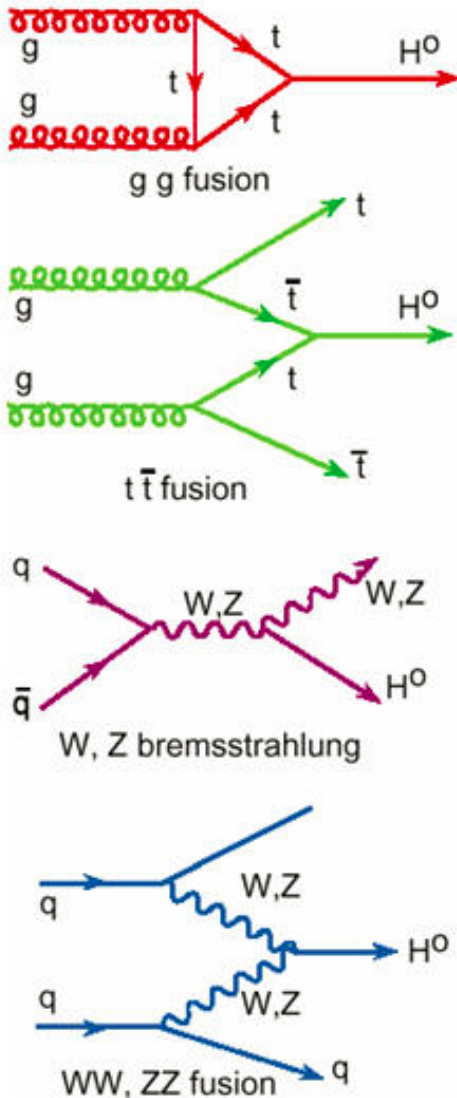
Collisions $\approx 10^7 - 10^9$ Hz

Higgs $\rightarrow ZZ^* \rightarrow 4l$ 通过对撞产生几率为10万亿分之一

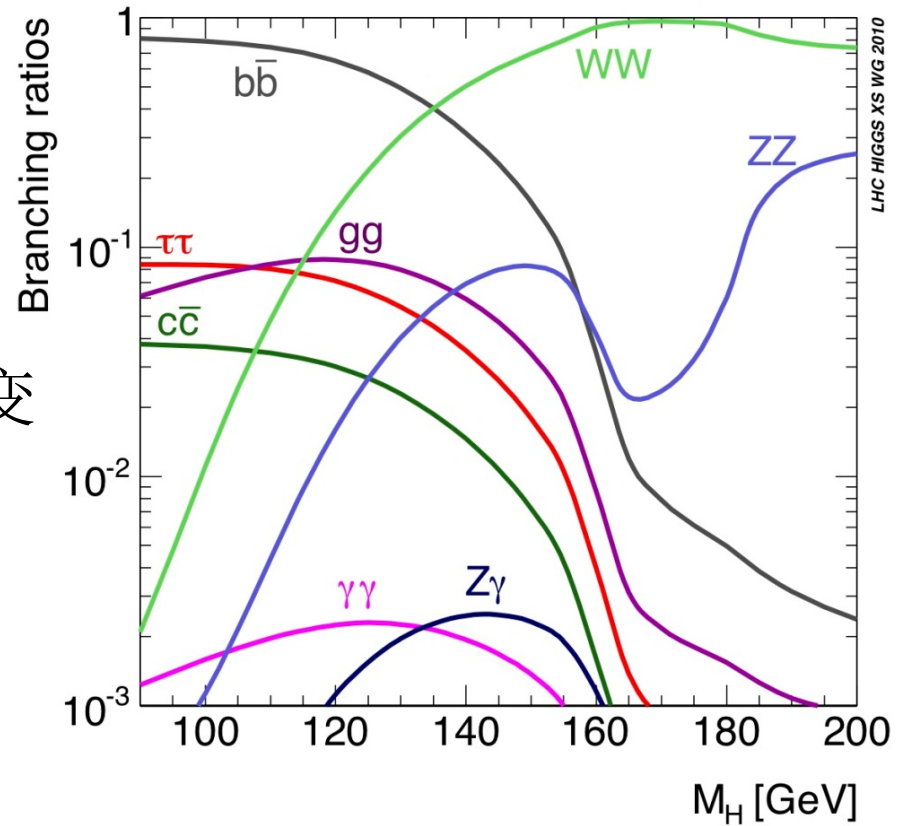
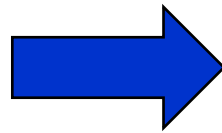
Selection of 1 in 10,000,000,000,000



Higgs粒子的产生和衰变

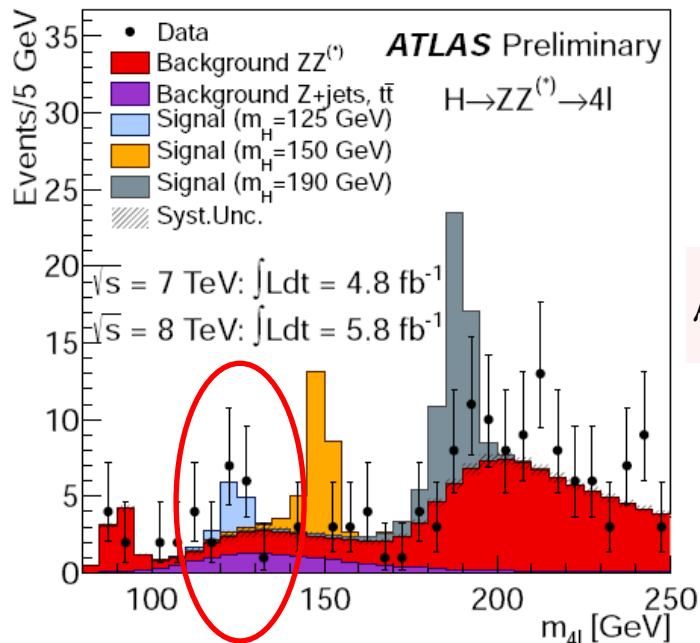
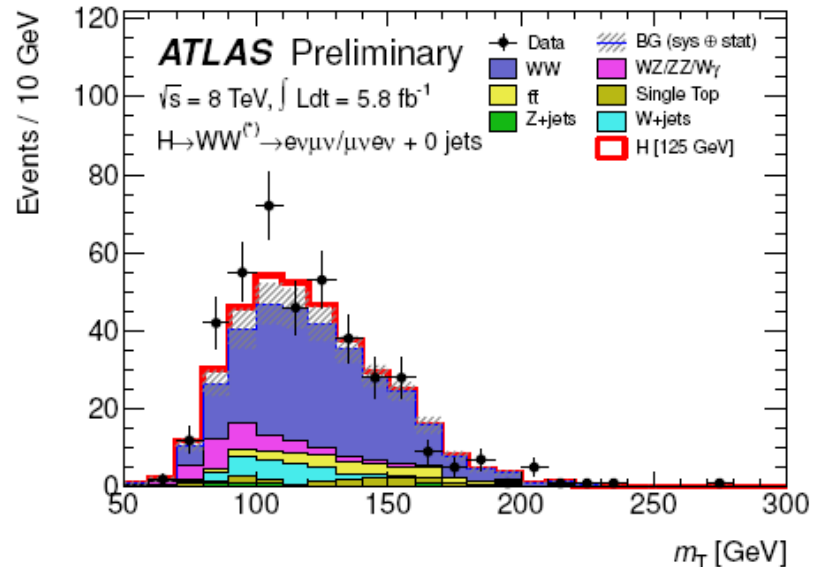
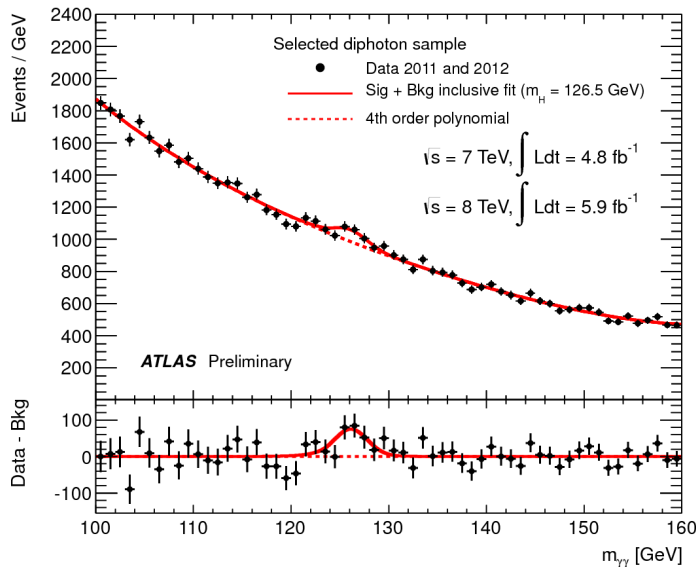


从产生到衰变

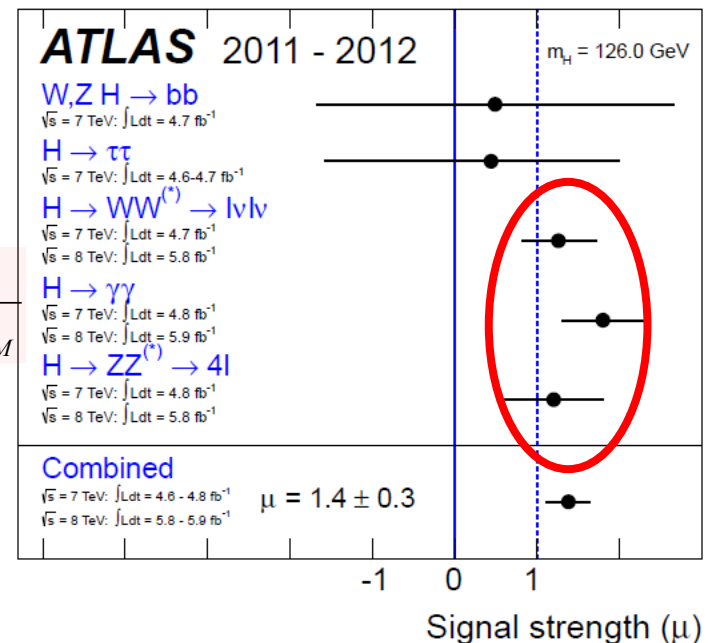


- Higgs粒子的产生需要较高能量，是稀有事件，在 10^{12} 个“事件”中大约能有一个Higgs粒子产生
- 在LHC上，Higgs可以被大量产生

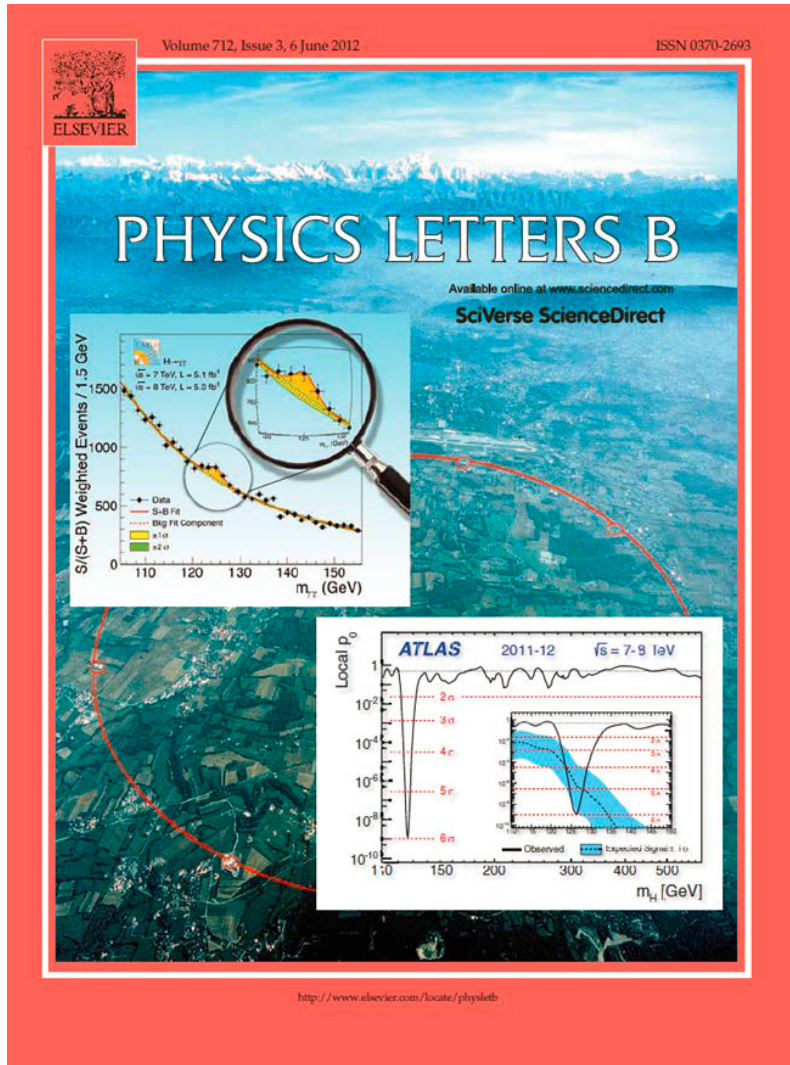
Higgs粒子的实验发现



$$\mu = \frac{\sigma \cdot Br}{(\sigma \cdot Br)_{SM}}$$



Higgs粒子的实验发现



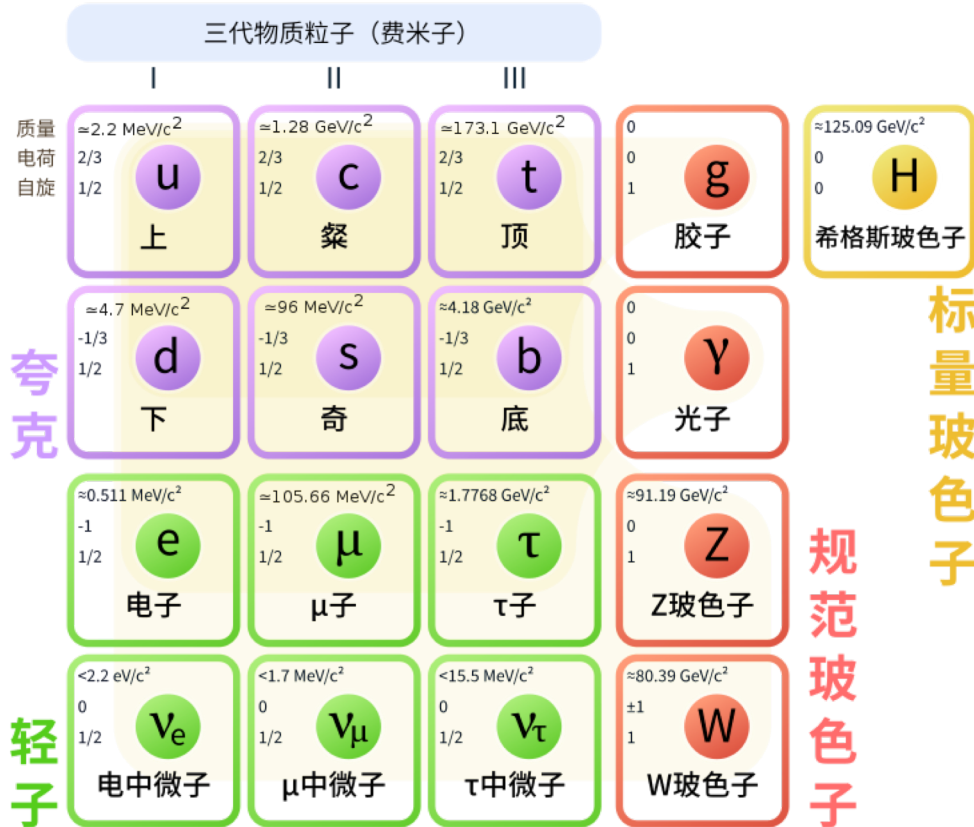
Phys. Lett. B 716 (2012) 1-29 (ATLAS)
Phys. Lett. B 716 (2012) 30-61 (CMS)



<http://www.sciencemag.org/site/special/btoy2012>

Higgs粒子的汤川耦合

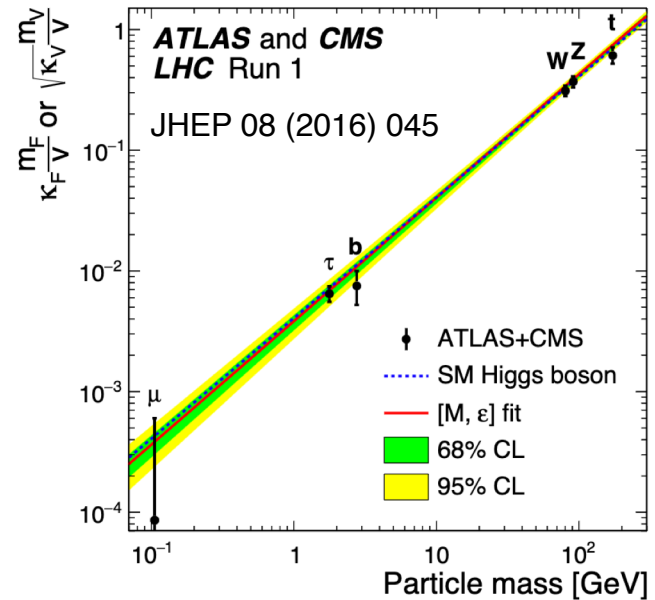
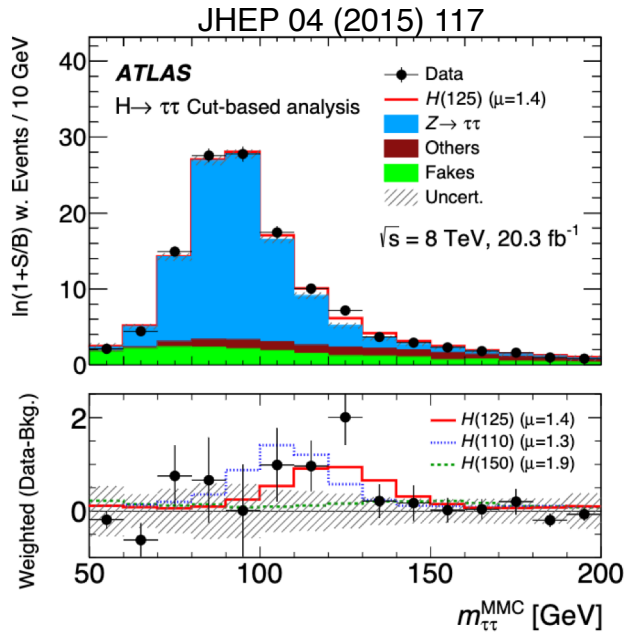
粒子物理标准模型



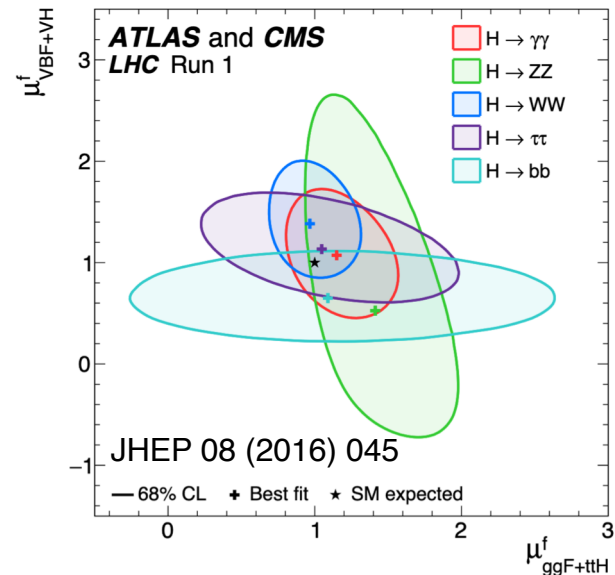
类型	电荷	自旋	质量
e	-1	1/2	0.5 MeV
ν _e	0	1/2	< 1.1 eV
μ	-1	1/2	106 MeV
ν _μ	0	1/2	< 0.2 MeV
τ	-1	1/2	1.77 GeV
ν _τ	0	1/2	< 18 MeV
u	+2/3	1/2	2.2 MeV
d	-1/3	1/2	4.7 MeV
c	+2/3	1/2	1.3 GeV
s	-1/3	1/2	96 MeV
t	+2/3	1/2	173.1 GeV
b	-1/3	1/2	4.2 GeV

Higgs通过汤川耦合赋予费米子质量: $\mathcal{L}_{\text{Yukawa}} = -g_i^L \bar{l}_{iR} \Phi^+ l_L^i - g_{ij}^d \bar{d}'_{iR} \Phi^+ q_L^j - g_i^u \bar{u}_{iR} \tilde{\Phi}^+ q_L^i + \text{h.c.}$

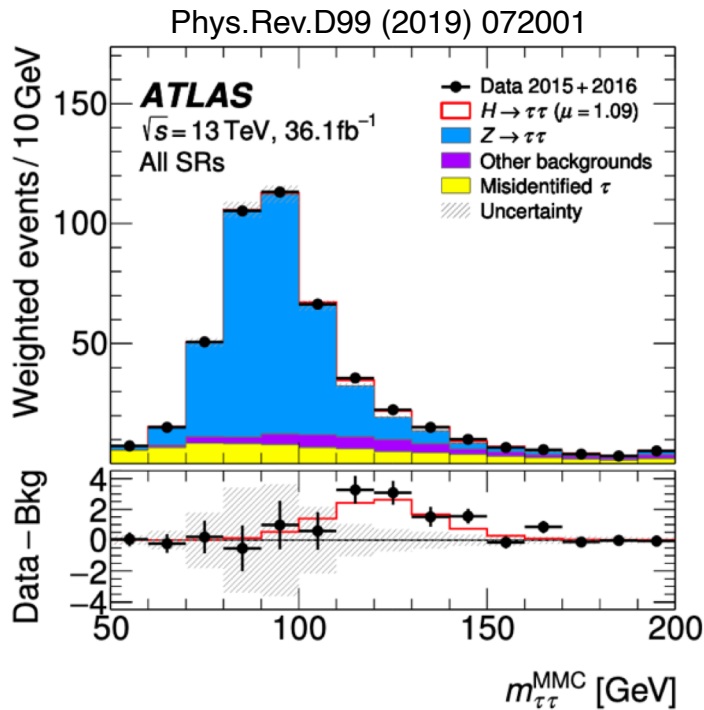
Higgs粒子的汤川耦合



- Higgs和费米子耦合强度正比于费米子质量 – tau轻子信号最有希望
 - 利用Run 1数据，ATLAS达到了 4.5σ 的显著度。与CMS结合后，达到了 5σ
- 欧洲核子研究中心总干事Rolf Heuer：
“...from the combined results the decay of the Higgs boson to tau particles is now observed with more than 5σ significance, which was not possible from CMS or ATLAS alone.”



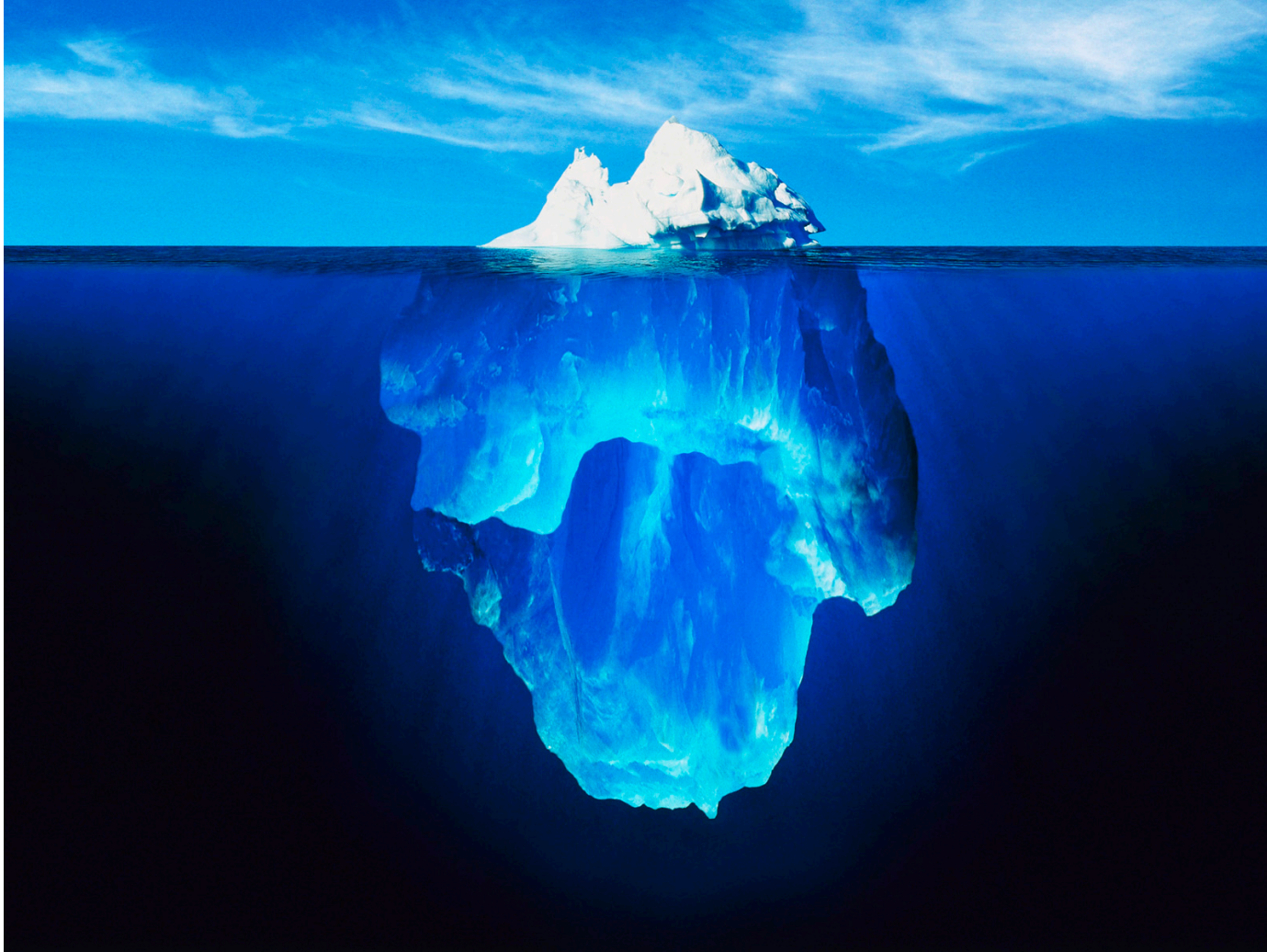
Higgs粒子与tau轻子的耦合



2018年，ATLAS在LHCP会议上宣布利用Run-2 36 fb⁻¹ 13万亿电子伏特对撞能量数据，在4.4倍标准差水平再次发现了这一过程（左图）。如果再与早期Run 1数据结合，则达到了6.4倍标准差水平，实现了在LHC（大型强子对撞机）上单个探测器对这一过程的再发现。

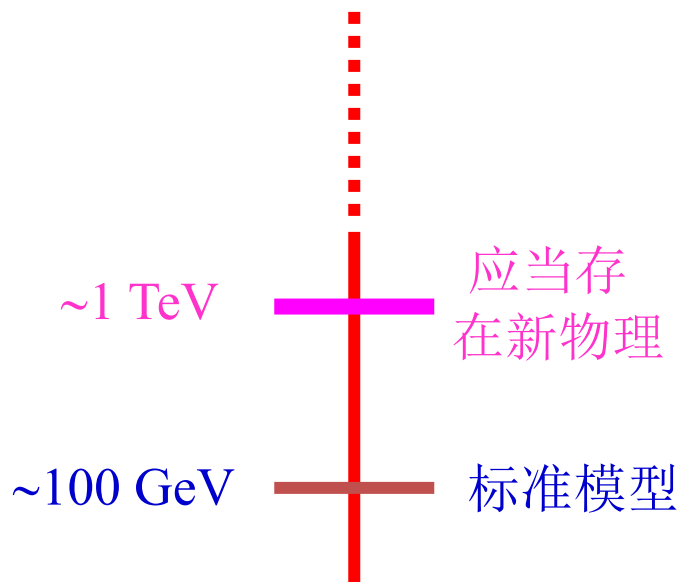
- 再次印证了Higgs场也是费米子质量的来源。2018年底，ATLAS实验合作组发言人Karl Jacobs评价到：“We have released a broad set of high-quality physics and performance results among which we may recall the memorable observation of Higgs boson couplings to fermions -to bottom and top quarks as well as to tau leptons-, ...”

Higgs粒子发现之后



理论疑难：精细调节问题

10^{16} GeV —— 大统一GUT



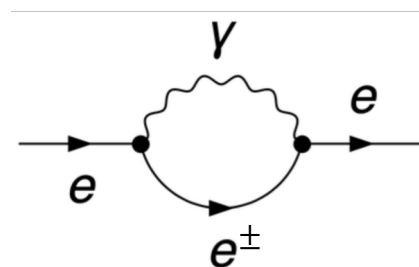
如果SM到GUT能标都正确，那么理论存在精细调节问题！

$$m_h^2 = m_0^2 - \delta m_h^2$$

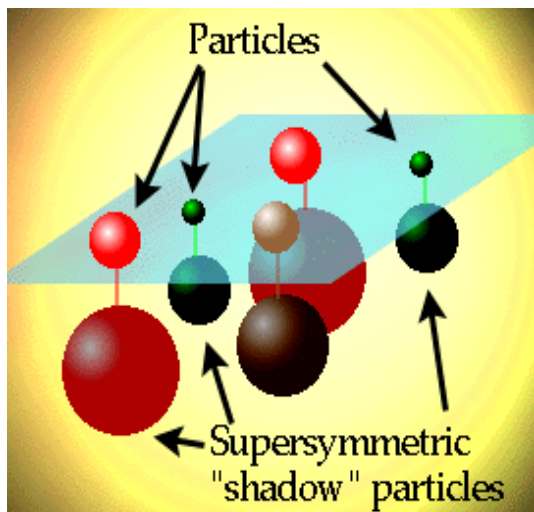
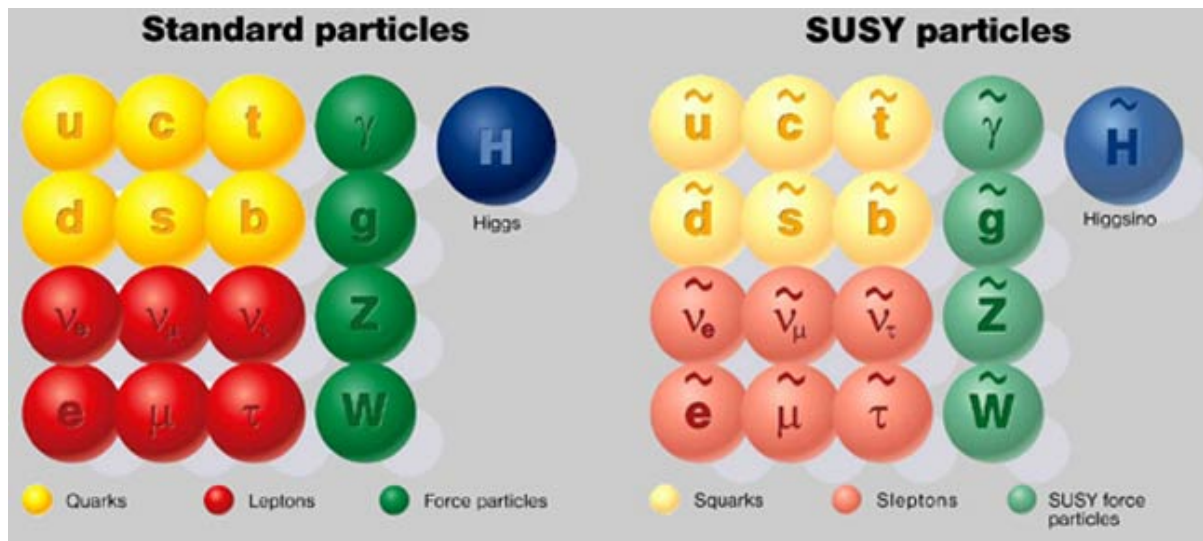
100 GeV 参数 Λ^2 修正

这就如同在地球上拿枪瞄准月球上的一只兔子。

相反，电子自能的量子修正包括正、负电子的贡献之和，即使到 10^{19} GeV的能标（Plank），修正也只有10%

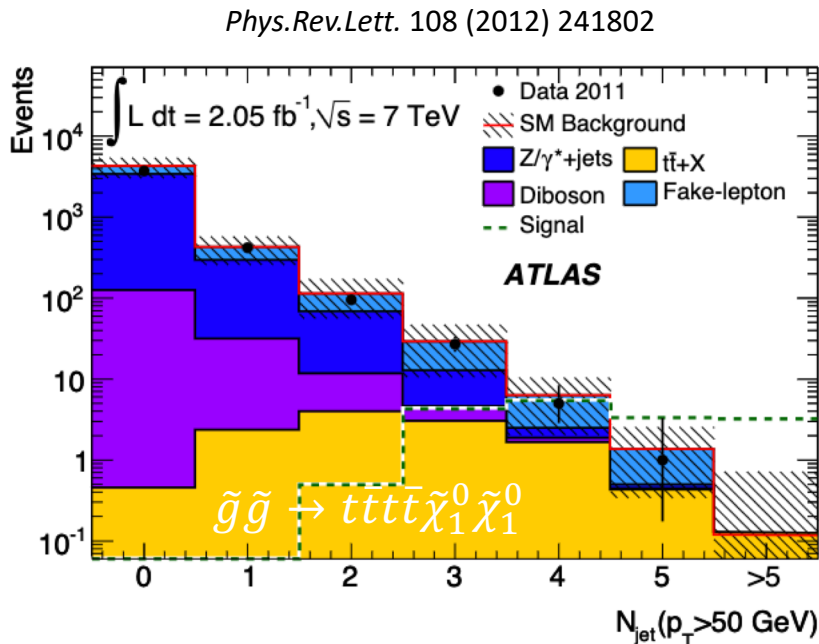
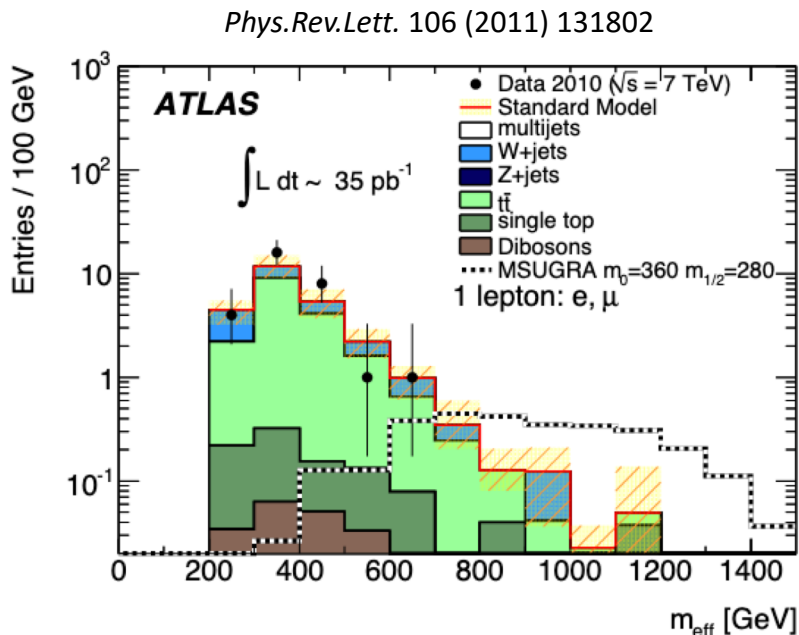


超对称理论



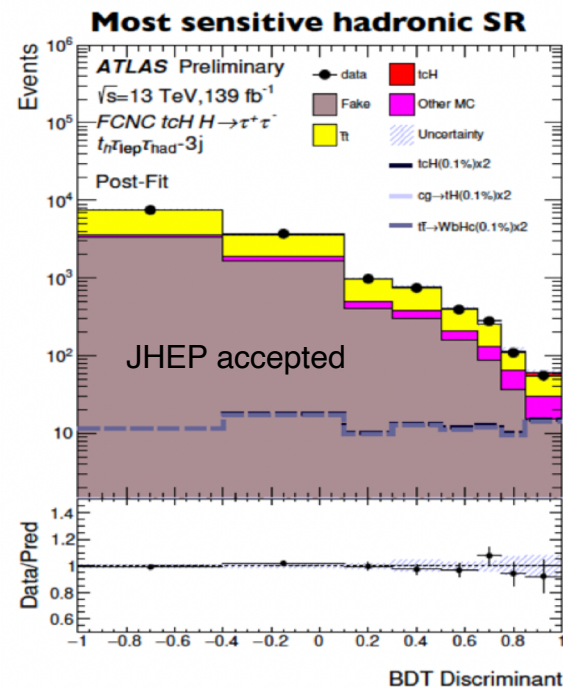
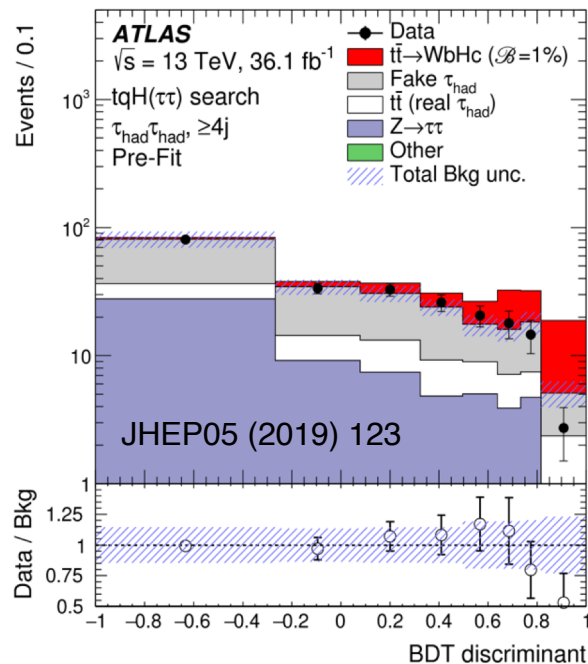
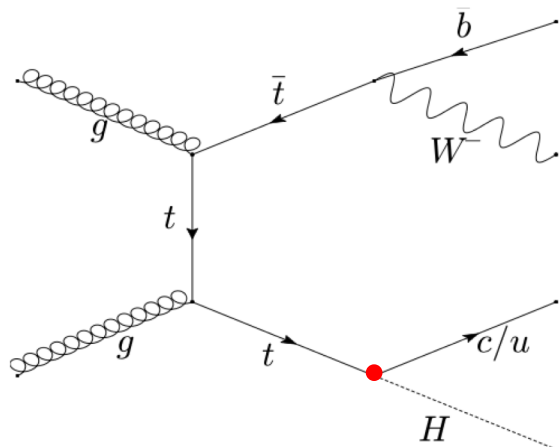
- 每个已知粒子都有一个“超对称”伙伴
- 有可能这些超对称粒子都很“重”所以难以被探测到
- 希格斯粒子质量没有精细调节问题
- 提供暗物质候选粒子 – 最轻的LSP粒子

在ATLAS上寻找超对称



- 实际上，得到ATLAS开机后第一批数据（7 TeV）后我们就开始找SUSY。遗憾的是，没有看到任何SUSY存在的迹象
- 由于SUSY粒子较重，产率对碰撞能量敏感，对数据亮度要求在其次。Run 2能量提升到13 TeV后，仍旧没有看到任何SUSY的信号
- 实验还在继续寻找，理论存活空间仍在

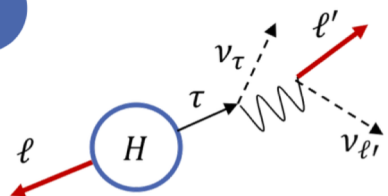
FCNC – 味改变的中性流



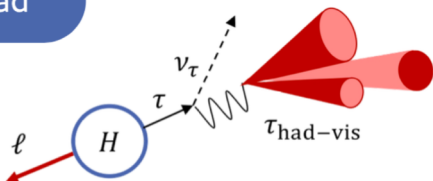
- 味改变的中性流过程在SM几乎为0，如果看到，则发现了新物理
- $t \rightarrow Hq$ 包含了基本粒子中最重的两个 – 顶夸克t和Higgs，对新物理敏感
- 我们分析了ATLAS的部分和全部的Run 2数据，没有发现FCNC信号的存在，给出了排除线

LFV - 轻子味道破坏

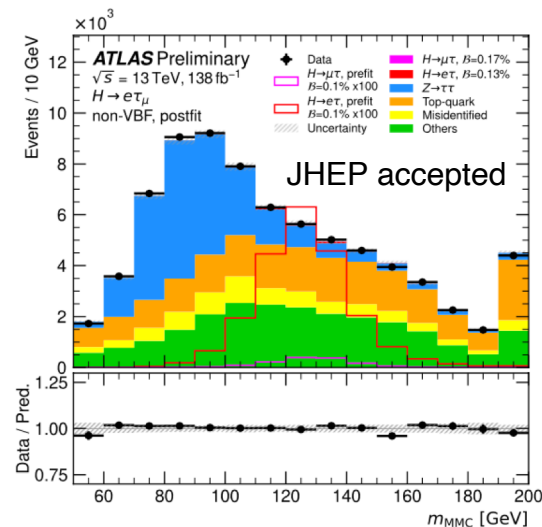
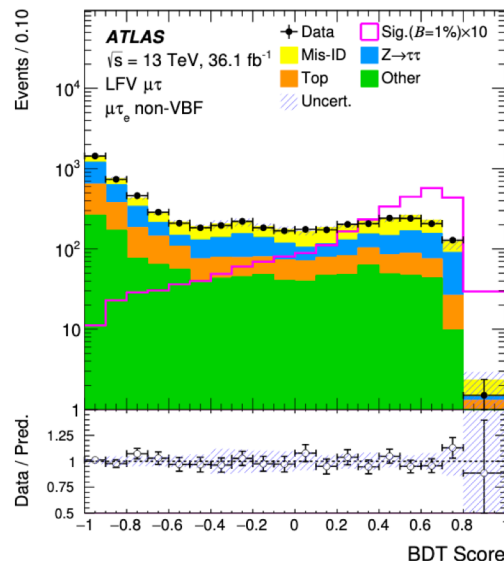
lelep



lephad



Phys. Lett. B 800 (2020) 135069



- 标准模型希格斯粒子没有诸如 $H \rightarrow e\tau$ 、 $H \rightarrow \mu\tau$ 等破坏轻子味道（LFV）的直接衰变，但某些超标准模型里有这种信号
- 探测Higgs的LFV衰变是对Higgs粒子新物理性质的一种探索
- 我们分析了ATLAS的部分和全部的Run 2数据，没有发现LFV信号的存在，给出了排除线

有效场论方法寻找重Higgs

有效6维算符:

$$\mathcal{L}_{HVV}^{(6)} = \sum_n \frac{f_n}{\Lambda^2} \mathcal{O}_n, \quad \Lambda = 5 \text{ TeV}$$

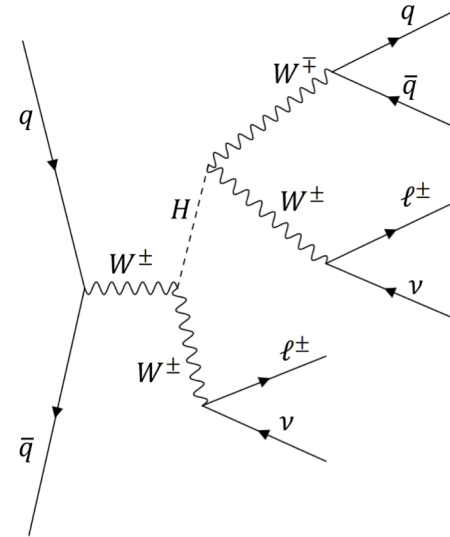
$$\mathcal{L}_{HWW}^{(6)} = \rho_{HG} m_W \frac{f_W}{2\Lambda^2} (W_{\mu\nu}^+ W^{-\mu} \partial^\nu H + h.c.)$$

$$- \rho_{HG} m_W \frac{f_{WW}}{\Lambda^2} W_{\mu\nu}^+ W^{-\mu\nu} H$$

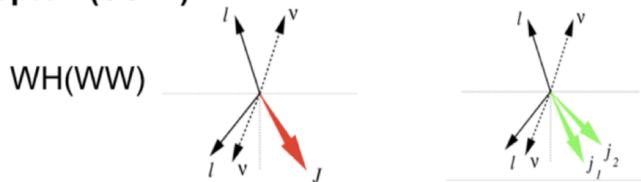
$$\mathcal{L}_{HZZ}^{(6)} = \rho_{HG} m_W \frac{c^2 f_W + s^2 f_B}{2c^2 \Lambda^2} Z_{\mu\nu} Z^\mu \partial^\nu H$$

$$- \rho_{HG} m_W \frac{c^4 f_{WW} + s^4 f_{BB}}{2c^2 \Lambda^2} Z_{\mu\nu} Z^{\mu\nu} H$$

$$s = \sin\theta_W, \quad c = \cos\theta_W$$

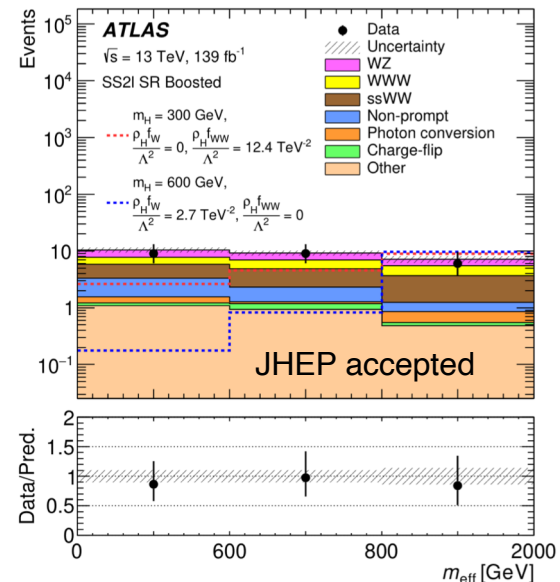


Same-sign 2 lepton (SS2L)



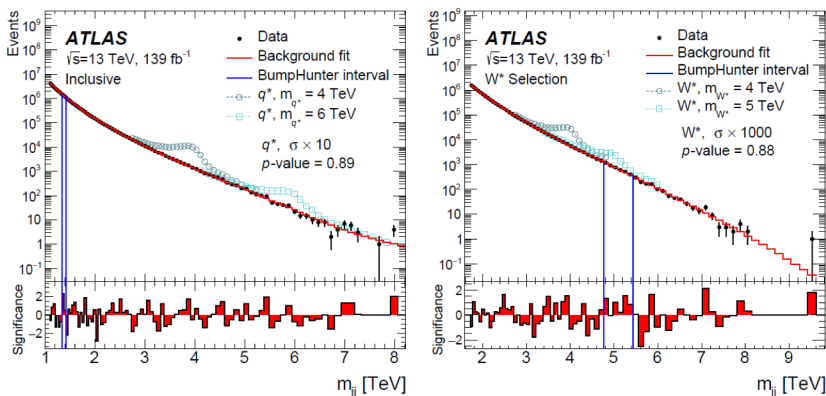
Observable: $M_{eff} = \sum p_T^{Lepton} + \sum p_T^{V-jets} + E_T^{miss}$

末态考虑两个同电荷轻子加上喷注
理论研究: arXiv:2211.02617



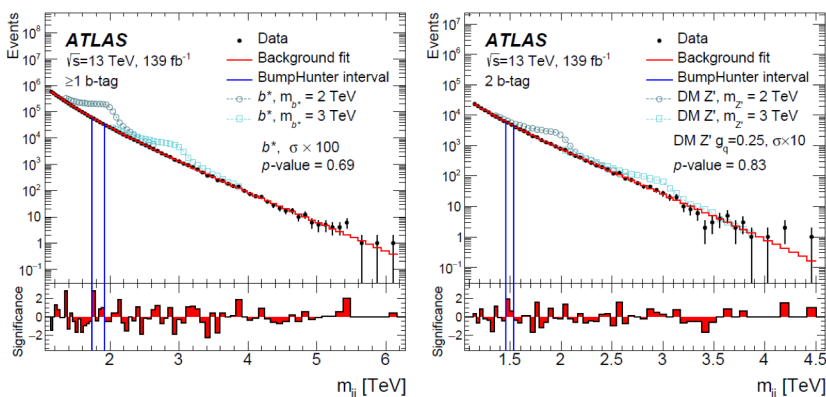
寻找双喷注共振态

JHEP03 (2020) 145



(a)

(b)



(c)

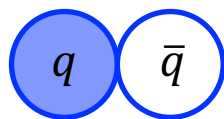
(d)

- 超出标准模型之外的新物理预言了能与胶子或者夸克耦合的重粒子的存在
- 这种粒子也可能与暗物质有关系
- SM强相互作用背景：双喷注不变质量谱是平滑下降的
- 如果有新粒子存在，则会体现为双喷注不变质量谱上的一个“鼓包”

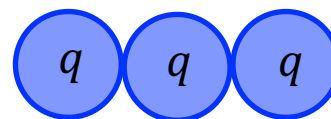
不同于其它研究，双喷注共振态的寻找是对新物理过程的直接寻找

夸克模型

传统夸克模型:

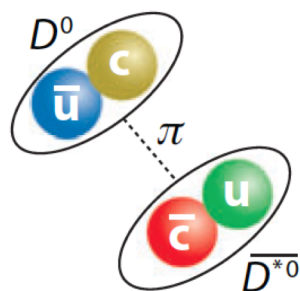


介子

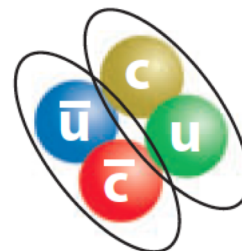


重子

分子态



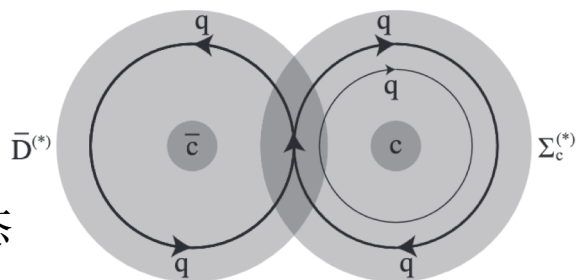
$D^0-\bar{D}^{*0}$ "molecule"



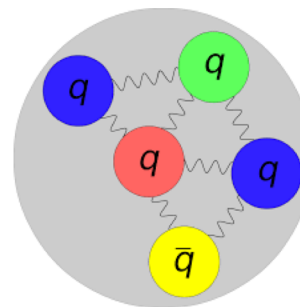
Diquark-diantiquark

紧致四夸克态

分子态



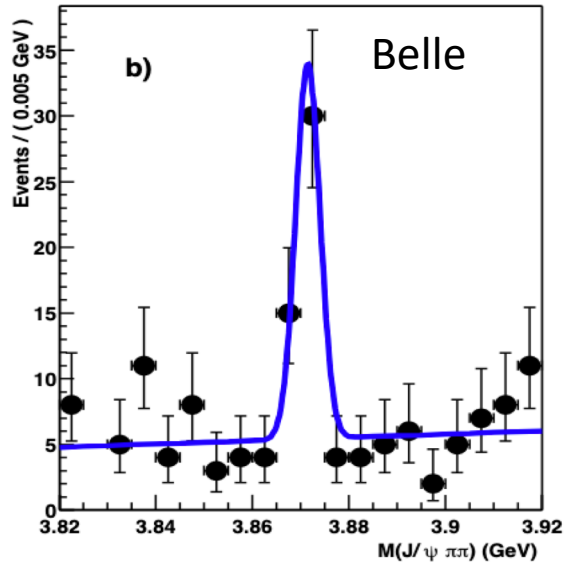
Commun. Theor. Phys. 74 125201



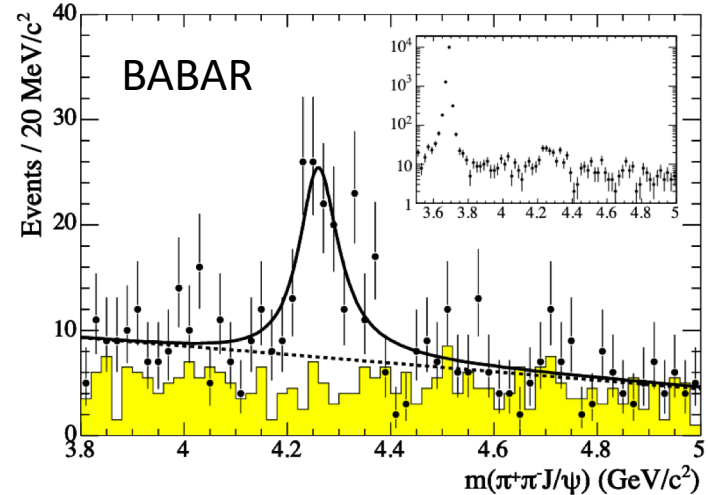
五夸克态

Hidden charm 四夸克态

[Phys. Rev. Lett 91 (2003) 262001]

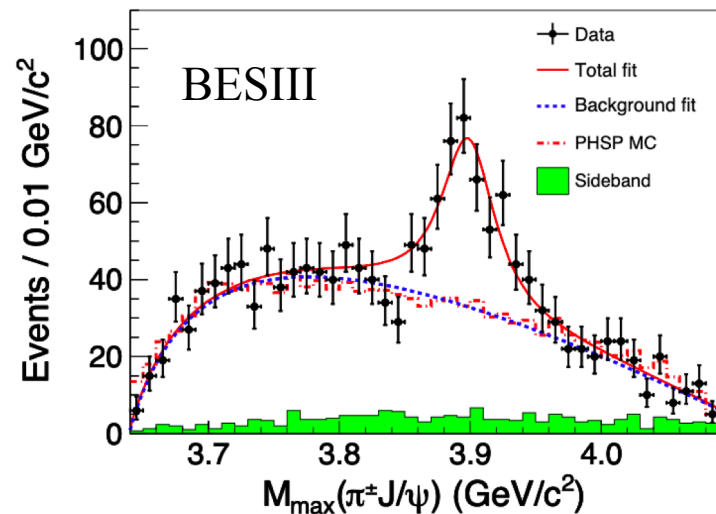


[Phys. Rev. Lett. 95 (2005) 142001]



[Phys.Rev.Lett. 110 (2013) 252001]

- X(3872) at Belle, Y(4260) at BABAR, Z_c⁺(3900) at BESIII, and later a number of XYZ states ...
- Charmed Tetraquark (TQ) state is often proposed for these LS
- Is it possible to have a 4-charm TQ?



All heavy 四夸克态

$$(cc)_3^* - (\bar{c}\bar{c})_3$$

L	S	J^{PC}	Mass (GeV)
1	0	1^{--}	6.55
	1	$0^{-+}, 1^{-+}, 2^{-+}$	
	2	$1^{--}, 2^{--}, 3^{--}$	
2	0	2^{++}	6.78
	1	$1^{+-}, 2^{+-}, 3^{+-}$	
	2	$0^{++}, 1^{++}, 2^{++}, 3^{++}, 4^{++}$	
3	0	3^{--}	6.98
	1	$2^{-+}, 3^{-+}, 4^{-+}$	
	2	$1^{--}, 2^{--}, 3^{--}, 4^{--}, 5^{--}$	

$$(cc)_6 - (\bar{c}\bar{c})_6^*$$

L	S	J^{PC}	Mass (GeV)
1	0	1^{--}	6.82
2	0	2^{++}	7.15
3	0	3^{--}	7.41



Fig. 2

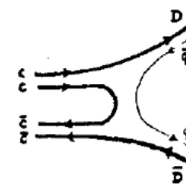


Fig.3(a)

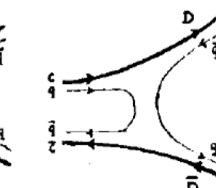


Fig.3(b)

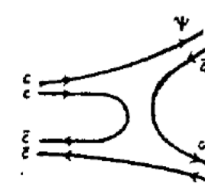


Fig.3(c)

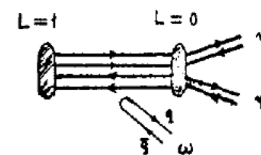
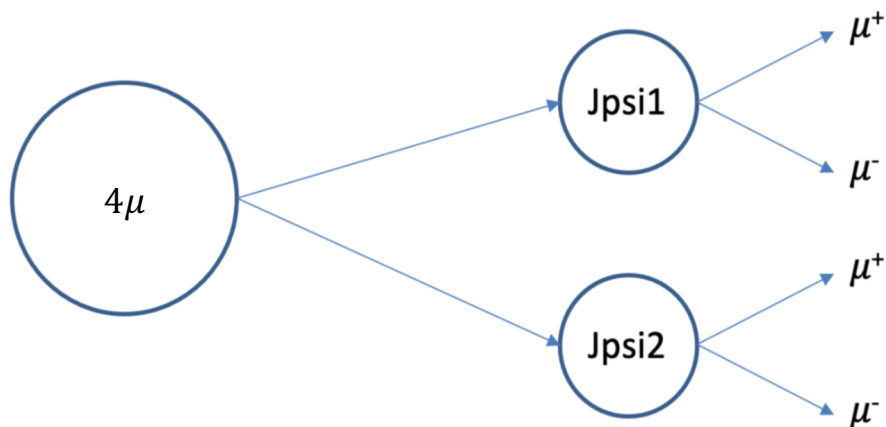


Fig.4

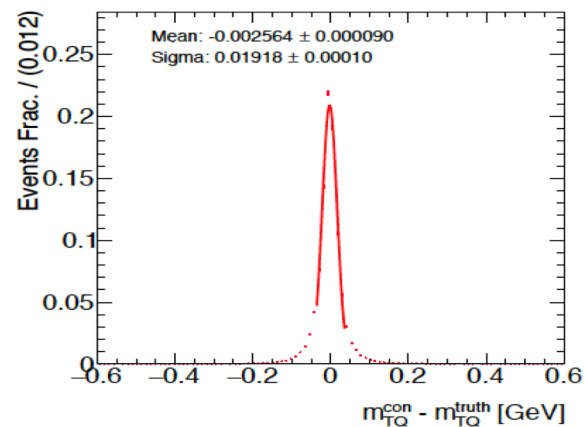
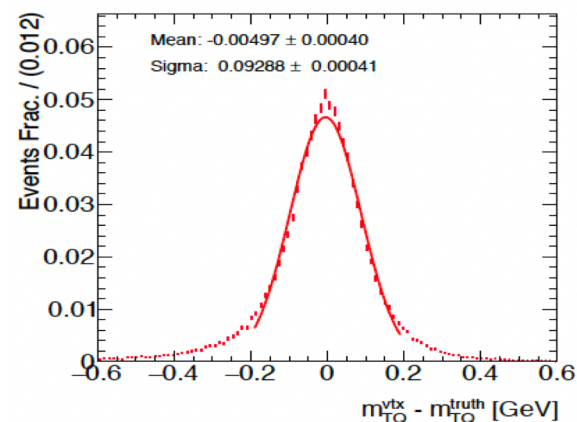
- 首次提到4c态(6.2 GeV, 1975): Prog. of Theo. Phys. Vol. 54, No. 2
- 首次计算4c态质量: Z. Phys. C 7 (1981) 317 (赵光达)

和重+轻夸克奇特态系统
很不一样

Reconstruction of 4μ vertex



- We first find vertex of J/ψ candidates with JpsiFinder Tool, Then use JpsiPlus2Tracks to fit 4μ to a common vertex. We use tool ReVertex to revertex two J/ψ tracks with a mass constraint, achieving a 4μ mass resolution of ~ 20 MeV
- Use sum of χ^2/N of two charmonia and 4μ vertices to select the best 4μ candidate per event



Signal and Backgrounds

➤ Signal process:

- Signal samples for process: $pp \rightarrow X \rightarrow \text{di-}J/\psi \rightarrow 4\mu$
 - TQ mass = 6.9 GeV, width = 0.1 GeV, spin = 0 with JHU

➤ Background processes:

- Prompt di- J/ψ background: Single Parton Scattering (SPS), Double Parton Scattering (DPS) with Pythia8
- Non prompt di- J/ψ background: $b\bar{b} \rightarrow J/\psi J/\psi$ with Pythia8
- Single J/ψ background:
 - Prompt or nonprompt J/ψ , plus fake muons from the primary vertex
- Non-peaking background containing no real J/ψ candidates

Collectively called “others”,
estimated from data

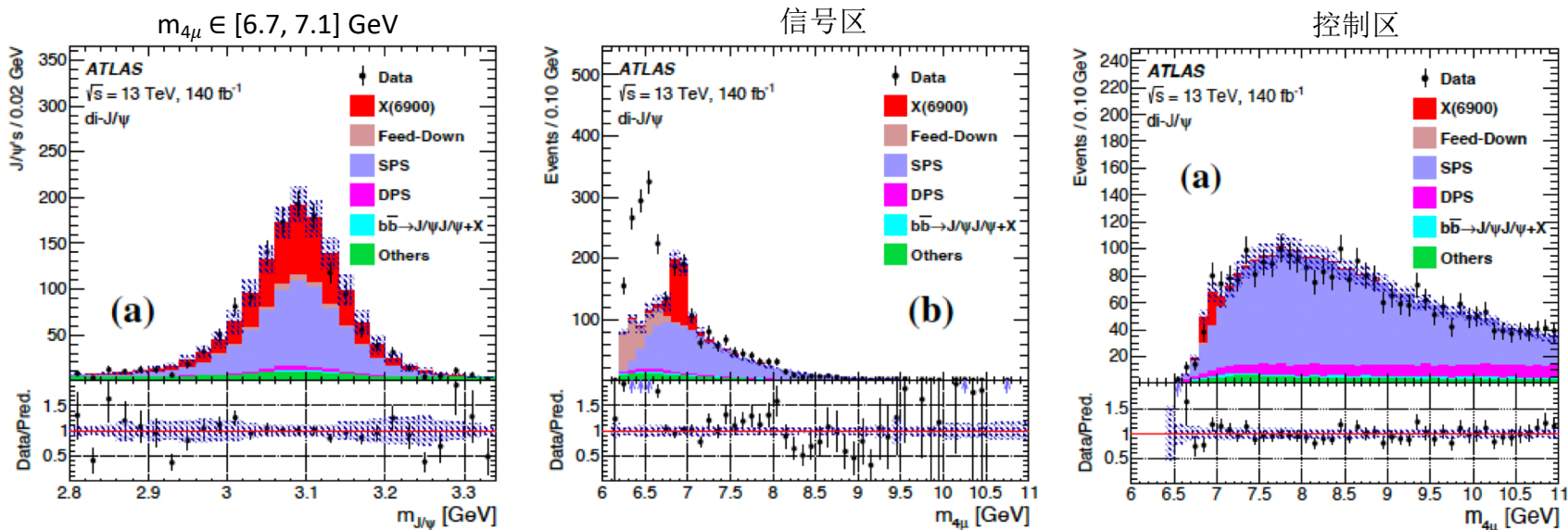
Offline event selection

➤ Selection cuts for different regions:

Signal region	SPS/DPS control region	non-prompt region
Di-muon or tri-muon triggers, Opposite charged muons from the same J/ψ or $\psi(2S)$ vertex, Loose muon ID, $p_T^{1,2,3,4} > 4, 4, 3, 3$ GeV and $ \eta_{1,2,3,4} < 2.5$ for the four muons $m_{J/\psi} \in \{2.94, 3.25\}$ GeV, or $m_{\psi(2S)} \in \{3.56, 3.80\}$ GeV, Loose vertex cuts $\chi_{4\mu}^2/N < 40$ and $\chi_{\text{di-}\mu}^2/N < 100$,		
Vertex $\chi_{4\mu}^2/N < 3$, $L_{xy}^{4\mu} < 0.2$ mm, $ L_{xy}^{\text{di-}\mu} < 0.3$ mm,		Vertex $\chi_{4\mu}^2/N > 6$,
$m_{4\mu} < 7.5$ GeV, $\Delta R < 0.25$ between charmonia	$7.5 \text{ GeV} < m_{4\mu} < 12.0$ GeV (SPS) $14.0 \text{ GeV} < m_{4\mu} < 25.0$ GeV (DPS)	$ L_{xy}^{\text{di-}\mu} > 0.4$ mm

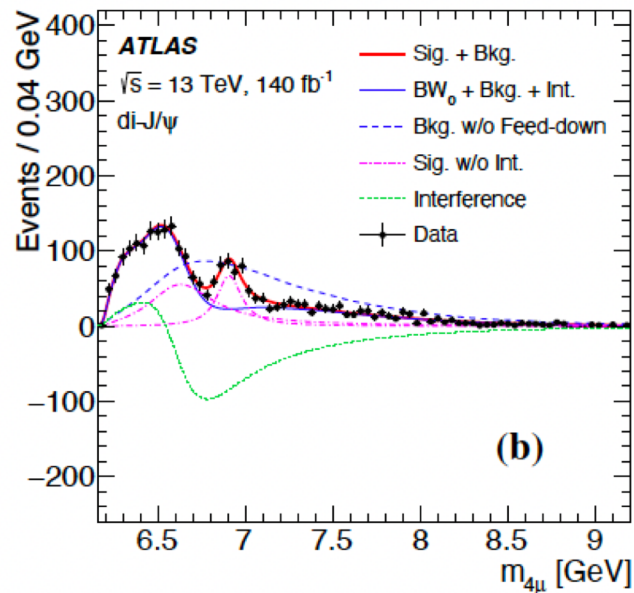
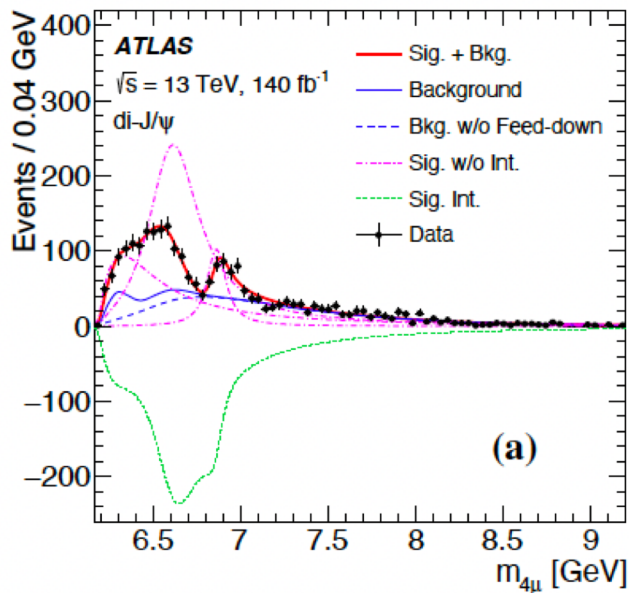
di- J/ψ channel

[arXiv:2304.08962]



- 主要的本底：SPS（单一部分子散射造成的双 J/ψ 本底）
- J/ψ 质量峰重建得很好，本底+信号与数据吻合
- 信号区规定用来拟合信号，控制区用来控制本底，尤其是SPS
- 包含了feed-down的本底（来自 $J/\psi + \psi(2S)$ channel）
- 6.9 GeV附近的峰与LHCb X6900一致

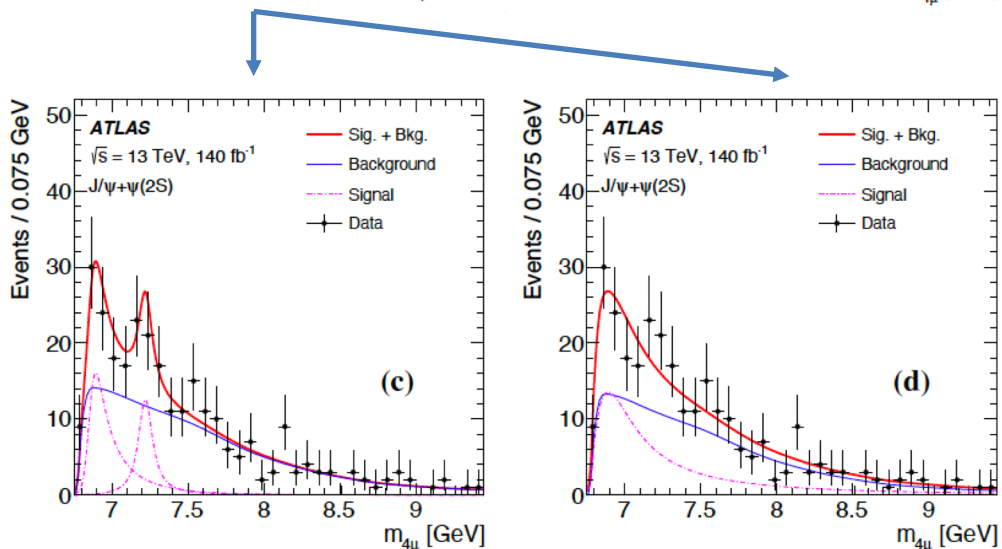
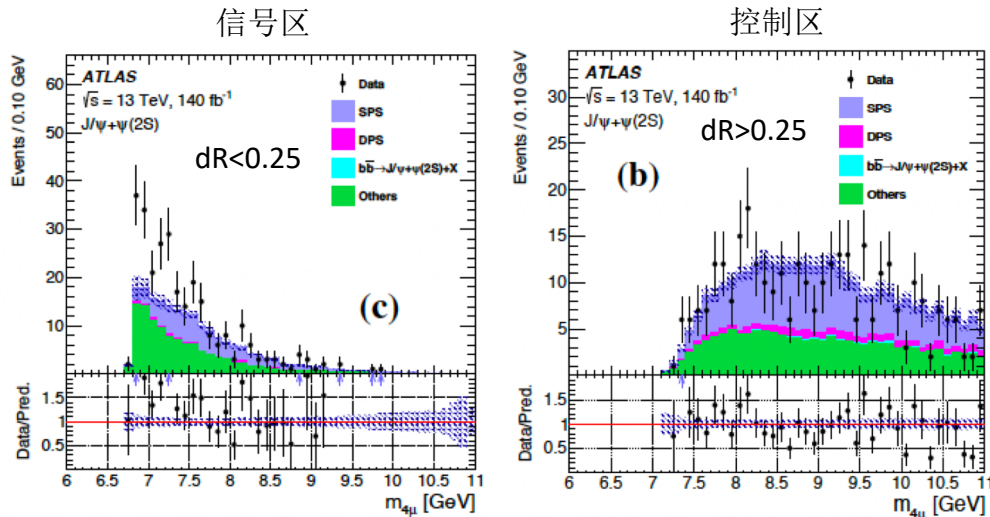
di- J/ψ channel



- 尝试了两个不同的拟合
 - 1) 3个相互干涉的共振峰(a)
 - 2) 一个共振峰和SPS干涉,
X6900独立共振峰(b)

di- J/ψ	model A	model B
m_0	$6.41 \pm 0.08^{+0.08}_{-0.03}$	$6.65 \pm 0.02^{+0.03}_{-0.02}$
Γ_0	$0.59 \pm 0.35^{+0.12}_{-0.20}$	$0.44 \pm 0.05^{+0.06}_{-0.05}$
m_1	$6.63 \pm 0.05^{+0.08}_{-0.01}$	—
Γ_1	$0.35 \pm 0.11^{+0.11}_{-0.04}$	—
m_2	$6.86 \pm 0.03^{+0.01}_{-0.02}$	$6.91 \pm 0.01 \pm 0.01$
Γ_2	$0.11 \pm 0.05^{+0.02}_{-0.01}$	$0.15 \pm 0.03 \pm 0.01$
$\Delta s/s$	$\pm 5.1\%^{+8.1\%}_{-8.9\%}$	—

J/ψ+ψ(2S) channel



- J/ψ+ψ(2S)是一个新的 channel, 可能是独立的, 也可能与双J/ψ channel有耦合效应
- 尝试了两个不同的拟合模型
 - 两个无干涉共振峰(c)
 - 一个共振峰(d)

J/ψ+ψ(2S)	model α	model β
m_3 or m	$7.22 \pm 0.03^{+0.01}_{-0.03}$	$6.96 \pm 0.05 \pm 0.03$
Γ_3 or Γ	$0.09 \pm 0.06^{+0.06}_{-0.03}$	$0.51 \pm 0.17^{+0.11}_{-0.10}$
$\Delta s/s$	$\pm 21\% \pm 14\%$	$\pm 20\% \pm 12\%$

CMS相关进展

- CMS实验观测到一个潜在的全粲四夸克粒子家族

- J/ψ - J/ψ 的不变质量谱中看到3个奇特强子
- X(6900): LHCb实验2020年发现, 本研究对其做了确认
- X(6600) 和 X(7300): 新粒子, 还未被其他实验观测到

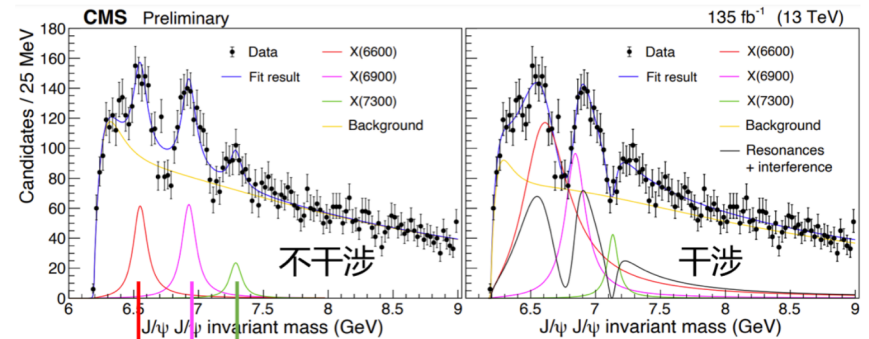
- 3粒子干涉模型更好地符合实验数据

- 它们可能具有相同的“自旋宇称”量子数因而来自于同一家族

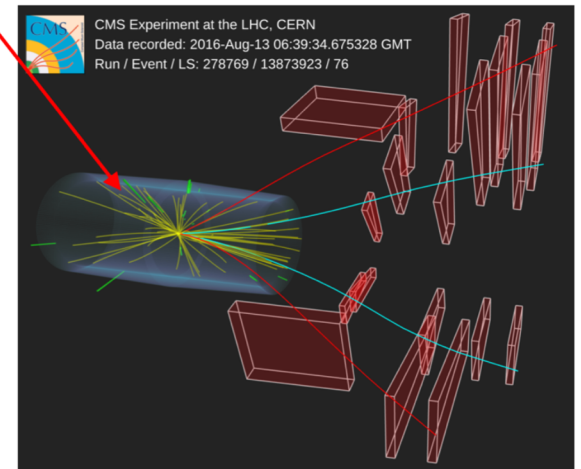
樱井奖得主Stanley Brodsky: “新发现的强子家族开辟了四夸克研究中一个重要的新领域。”

CMS实验B物理召集人Riccardo Manzoni: “中国团队在这一成果中扮演了主要角色。”

赵光达院士: “我十分高兴中国的实验粒子物理学家们在这项发现中起到了主导作用。”



X(6600)
X(6900)
X(7300)



CMS Experiment at the LHC, CERN
Data recorded: 2016-Aug-13 06:39:34.675328 GMT
Run / Event / LS: 278769 / 13873923 / 76

Angular analysis for spin and parity

In helicity formalism, for a particle of spin (J, M) decaying into two particles in (θ, φ) direction with helicities (λ, ν) , the decay amplitude can be expressed as

$$\begin{aligned}\mathcal{M}_{\lambda\nu}^J(\theta, \varphi; M) &\propto \langle \theta \varphi \lambda \nu | JM \lambda \nu \rangle \langle JM \lambda \nu | \mathcal{M} | JM \rangle \\ &\propto F_{\lambda\nu}^J D_{M\delta}^{J*}(\varphi, \theta, 0)\end{aligned}$$

where $\delta = \lambda - \nu$, $D_{M\delta}^{J*}$ is the Wigner D-function and $F_{\lambda\nu}^J \propto \langle JM \lambda \nu | \mathcal{M} | JM \rangle$. If parity is conserved, we have

$$F_{\lambda\nu}^J = \eta_J \eta_1 \eta_2 (-1)^{J-s_1-s_2} F_{-\lambda, -\nu}^J$$

where η_J, η_1, η_2 are the intrinsic parities of mother and two daughters, and for identical daughters (e.g., di- J/ψ), we have in addition

$$F_{\lambda\nu}^J = (-1)^J F_{\nu\lambda}^J$$

In the case of identical particles, the final state should be also symmetrized

$$\mathcal{M}^J(\theta, \varphi; M) \propto {}_s \langle \theta \varphi \lambda \nu | JM \lambda \nu \rangle {}_s \langle JM \lambda \nu | \mathcal{M} | JM \rangle$$

Helicity formalism and partial waves

With the symmetrization implemented, we have

$$\mathcal{M} \propto \sum_{\lambda \geq \nu} F_{\lambda\nu}^J D_{M\delta}^{J*}(\varphi, \theta, 0) c_{\lambda\nu} [D_{\lambda\delta_1}^{1*}(\varphi_1, \theta_1, 0) D_{\nu\delta_2}^{1*}(\varphi_2, \theta_2, 0) + D_{\nu\delta_1}^{1*}(\varphi_1, \theta_1, 0) D_{\lambda\delta_2}^{1*}(\varphi_2, \theta_2, 0)]$$

Note that θ, φ are defined in the rest frame of TQ, while θ_1, φ_1 (θ_2, φ_2) are defined for, e.g. μ^+ , in the rest frame of J/ψ_1 (J/ψ_2).

The helicity amplitude can be broken down into different total orbital (L) and spin (S) angular momentum components (partial wave decomposition):

$$F_{\lambda\nu}^J = \sum_{LS} \sqrt{\frac{2L+1}{2J+1}} \begin{bmatrix} L & S & J \\ 0 & \delta & \delta \end{bmatrix} \begin{bmatrix} s_1 & s_2 & S \\ \lambda & -\nu & \delta \end{bmatrix} G_{LS}^J$$

where the 3-column numbers in brackets are CG coefficients. F and G satisfy

$$\sum_{LS} |G_{LS}^J|^2 = \sum_{\lambda\nu} |F_{\lambda\nu}^J|^2$$

If parity is conserved, we should have $\eta_J = \eta_1 \eta_2 (-1)^L$. In addition, for two identical final state particles, L+S must be even.

Example: hypotheses 0^+ and 0^-

- For the case of $0^+ \rightarrow 1^- 1^-$, only $L=S=0$, or $L=S=2$ are allowed, and

$$F_{11}^0 = \frac{1}{\sqrt{3}} G_{00}^0 + \frac{1}{\sqrt{6}} G_{22}^0, \quad F_{-1,-1}^0 = F_{11}^0, \quad F_{00}^0 = -\frac{1}{\sqrt{3}} G_{00}^0 + \sqrt{\frac{2}{3}} G_{22}^0, \quad \text{all other } F_{\lambda\nu}^0 = 0.$$

$$\mathcal{M} \propto F_{11}^0 [e^{i(\varphi_1 + \varphi_2)} d_{1\delta_1}^1(\theta_1) d_{1\delta_2}^1(\theta_2) + e^{-i(\varphi_1 + \varphi_2)} d_{-1\delta_1}^1(\theta_1) d_{-1\delta_2}^1(\theta_2)] + F_{00}^0 d_{0\delta_1}^1(\theta_1) d_{0\delta_2}^1(\theta_2)$$

$$\sum_{\delta_1 \delta_2} |\mathcal{M}|^2 \propto |F_{11}^0|^2 [(\cos^2 \theta_1 \cos^2 \theta_2 + 1) \cos^2(\varphi_1 + \varphi_2) + (\cos^2 \theta_1 + \cos^2 \theta_2) \sin^2(\varphi_1 + \varphi_2)] \\ + |F_{00}^0|^2 \sin^2 \theta_1 \sin^2 \theta_2 + \frac{1}{2} \text{Re}(F_{11}^0 F_{00}^{0*}) \sin 2\theta_1 \sin 2\theta_2 \cos(\varphi_1 + \varphi_2)$$

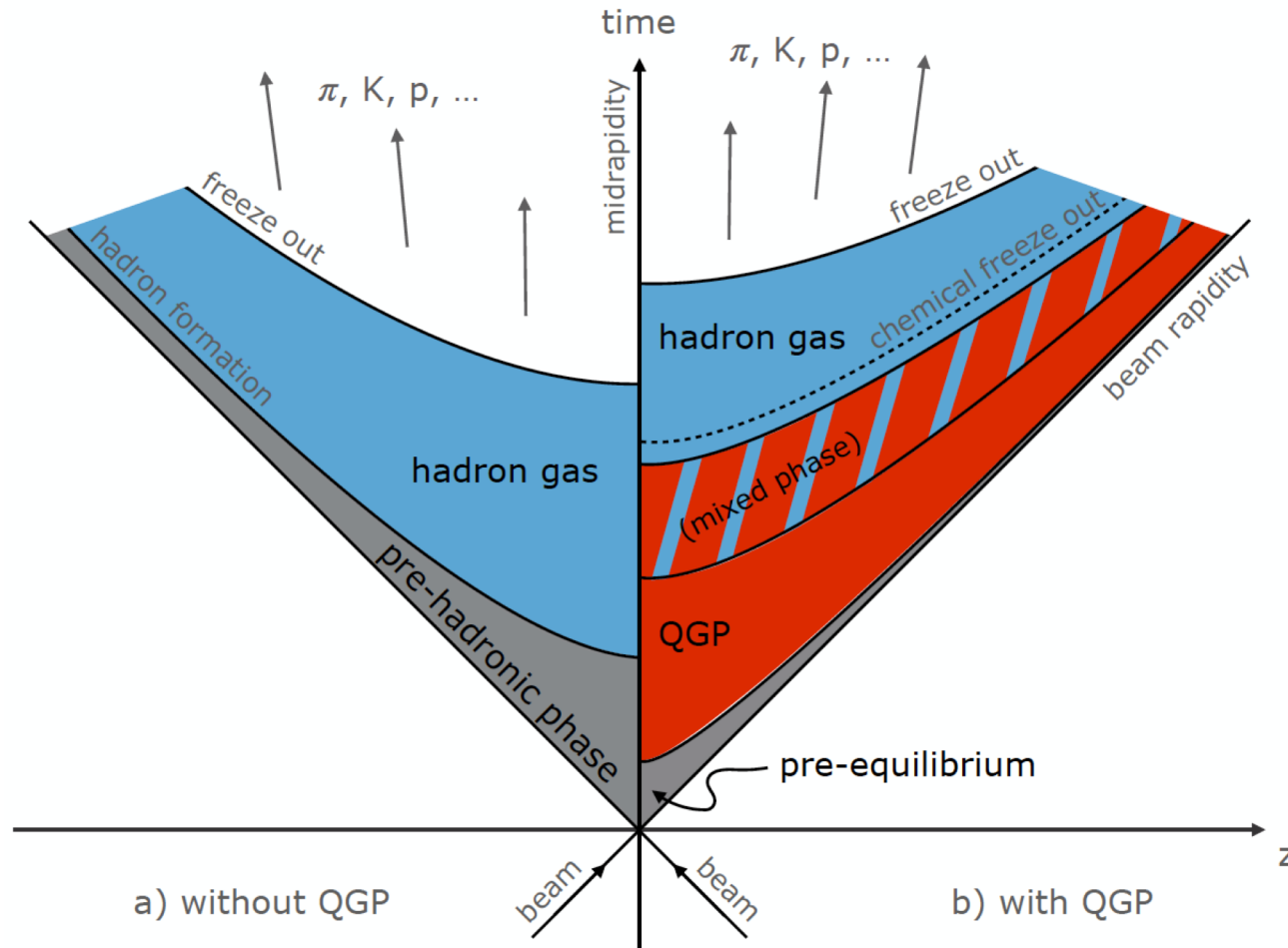
- For the case of $0^- \rightarrow 1^- 1^-$, only $L=S=1$ is allowed, and

$$F_{11}^0 = -\frac{1}{\sqrt{2}} G_{11}^0, \quad F_{-1,-1}^0 = -F_{11}^0, \quad \text{all other } F_{\lambda\nu}^0 = 0.$$

$$\mathcal{M} \propto \frac{1}{\sqrt{2}} G_{11}^0 [e^{-i(\varphi_1 + \varphi_2)} d_{-1\delta_1}^1(\theta_1) d_{-1\delta_2}^1(\theta_2) - e^{i(\varphi_1 + \varphi_2)} d_{1\delta_1}^1(\theta_1) d_{1\delta_2}^1(\theta_2)]$$

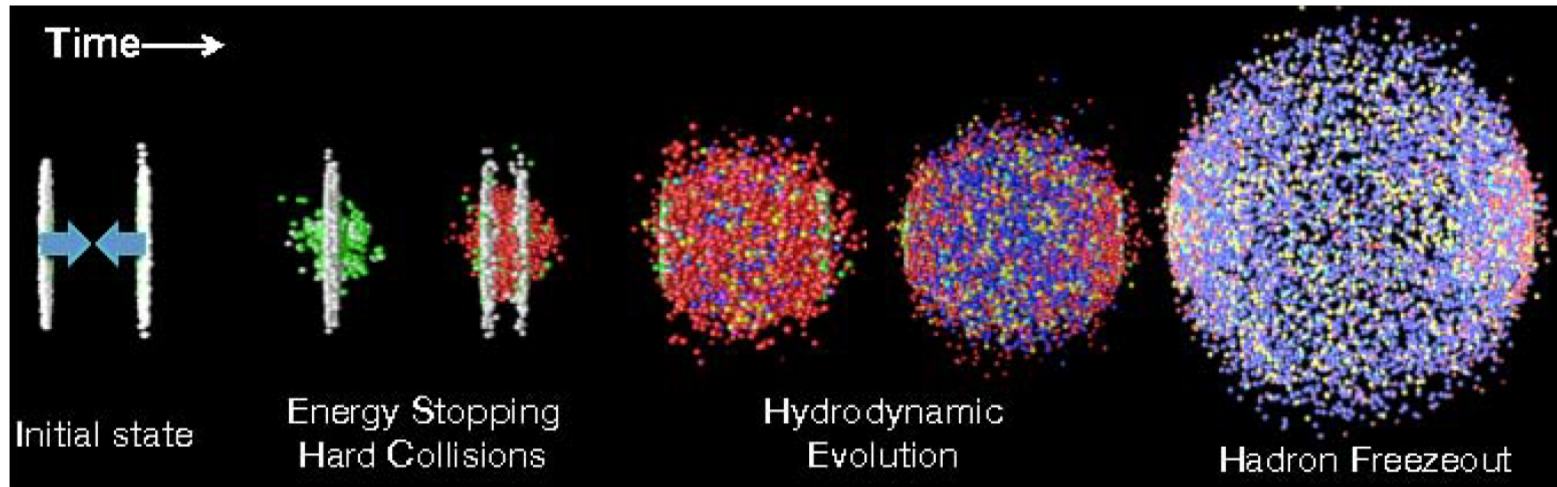
$$\sum_{\delta_1 \delta_2} |\mathcal{M}|^2 \propto \frac{1}{4} |G_{11}^0|^2 [(1 + \cos^2 \theta_1)(1 + \cos^2 \theta_2) - \sin^2 \theta_1 \sin^2 \theta_2 \cos 2(\varphi_1 + \varphi_2)]$$

Heavy Ion collisions



- Small system collisions, such as p-p and p-A, are not expected to have QGP
- Large system collisions, such as A-A, are expected to have QGP

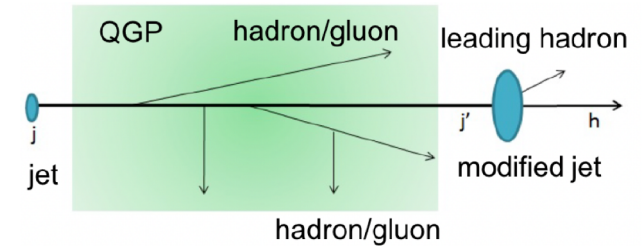
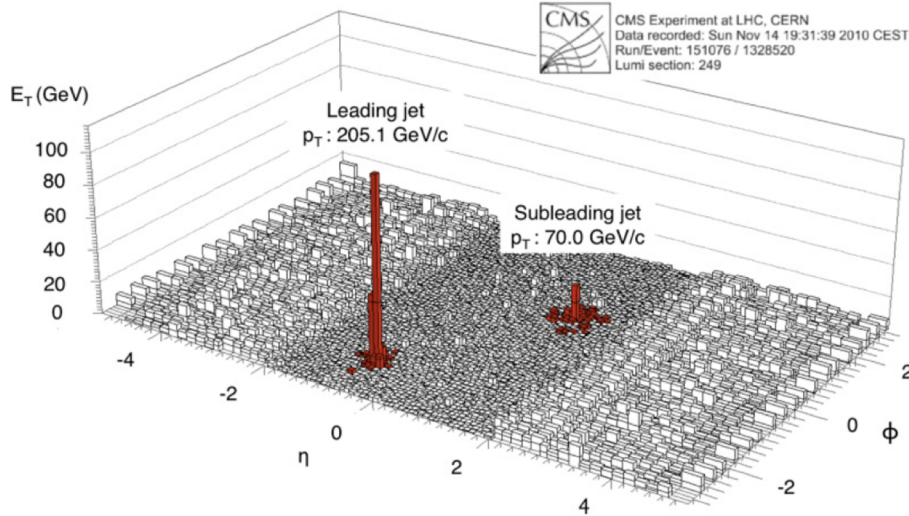
Heavy Ion collisions



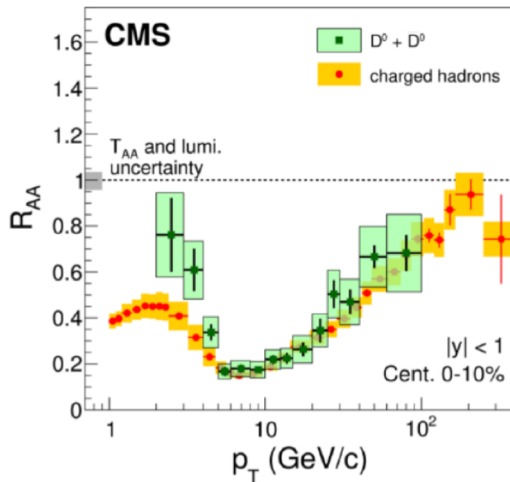
QGP effects in heavy ion collisions:

- Strangeness enhancement: Strange quarks can be produced thermally and coalesce to hadrons.
- Jet quenching: Modification of hadrons p_T spectrum and asymmetry in back-to-back jets production
- Heavy quarkonium suppression: In QGP the bound of the quark anti-quark pair is looser as a result of the Debye screening

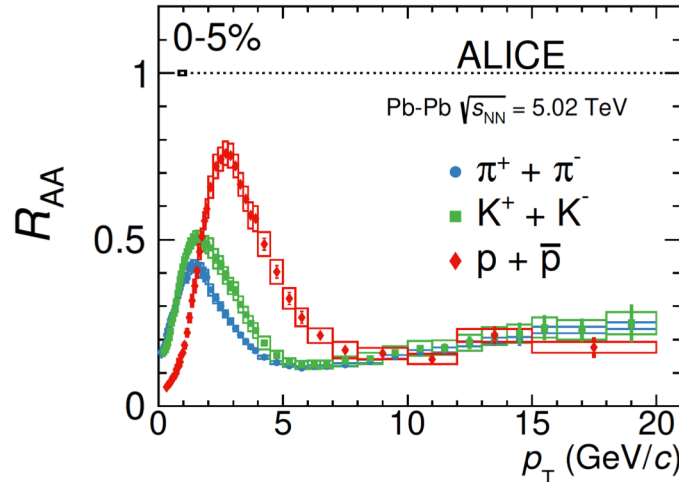
Jet quenching



Phys. Lett. B 782 (2018) 474

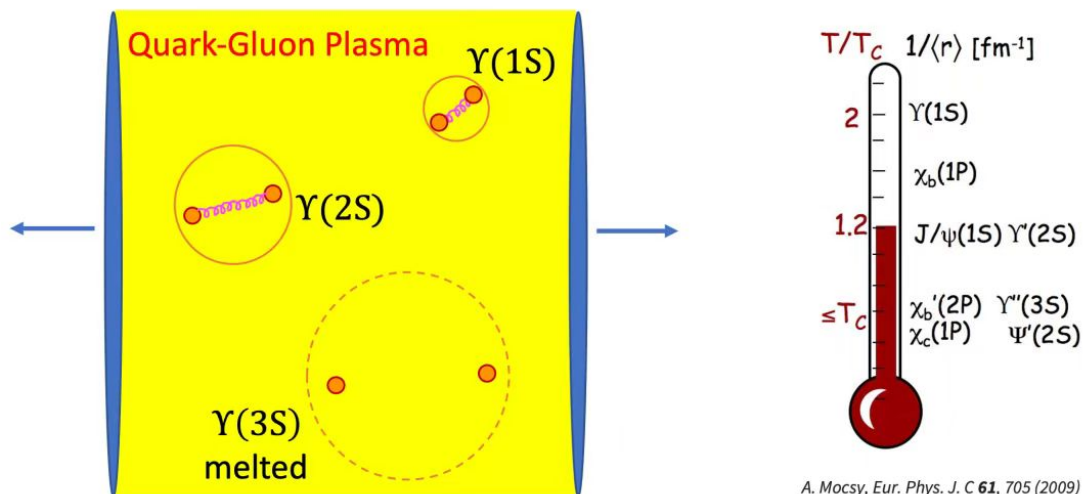


Phys. Rev. C 101 (2020) 044907

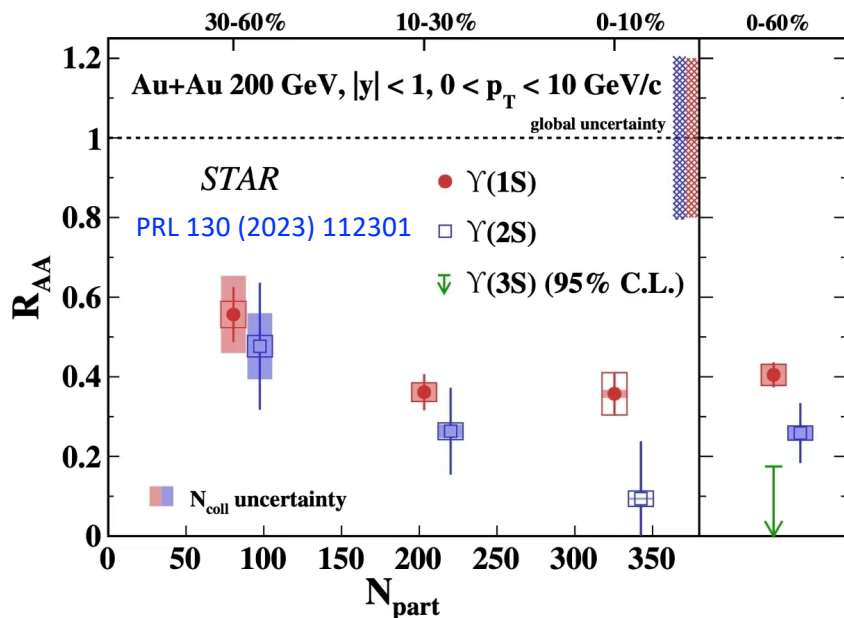


R_{AA} : relative production rates in A-A and p-p collisions (A-A is normalized to per nucleon-nucleon binary collision)

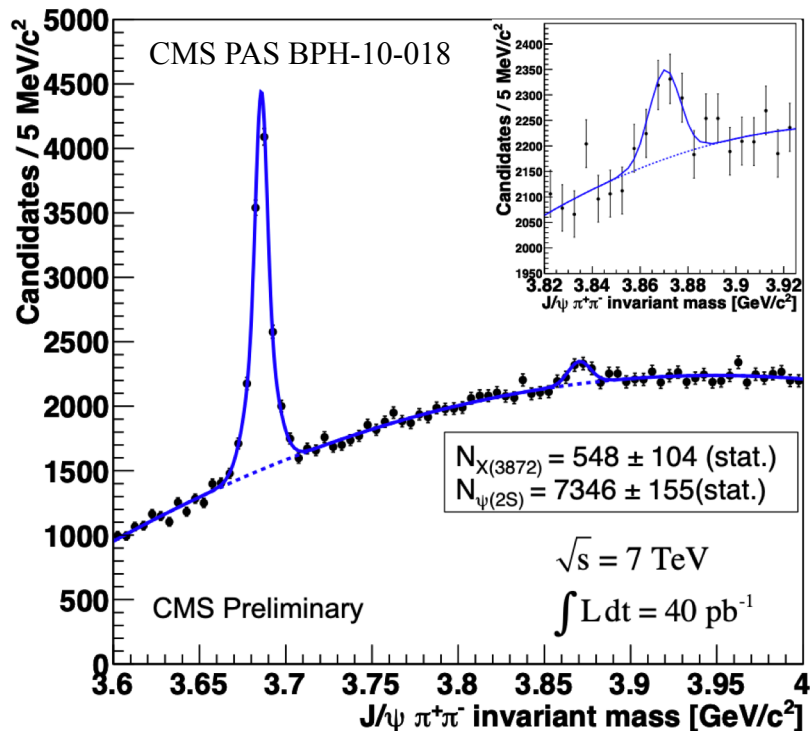
Heavy quarkonium suppression



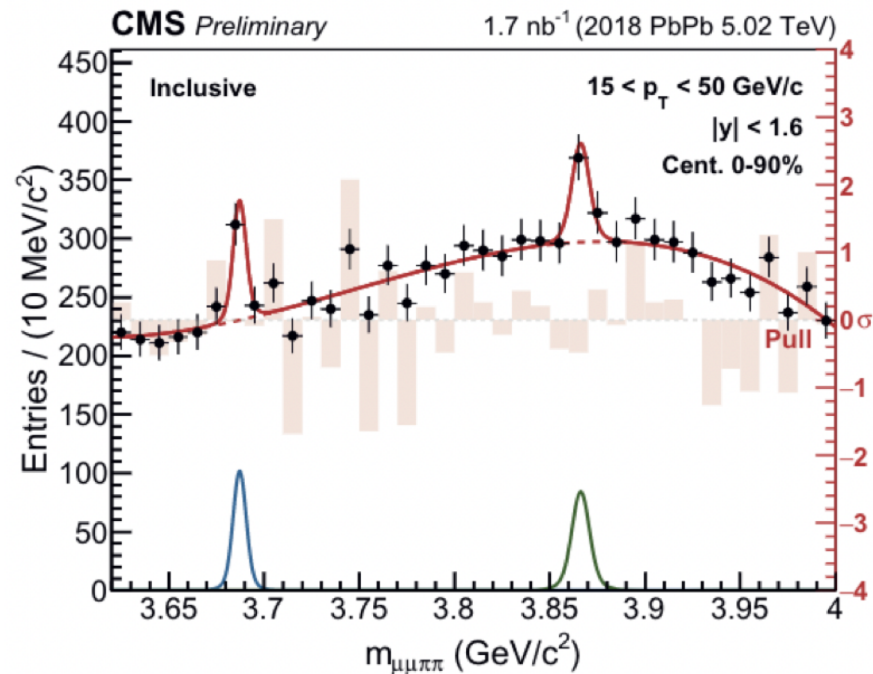
在QGP中，强相互作用的德拜屏蔽效应改变了底夸克和反底夸克之间的相互作用势，使得弱束缚（大尺度）的底夸克偶素激发态更容易解除束缚而造成产额压低，这被称为“顺次熔解”或“顺次压低”（左图）。由于各个态产额压低的程度对QGP的温度（决定了德拜屏蔽长度）非常敏感，因此这些态产额压低的测量也被称为QGP的“温度计”



Tetraquark in Heavy Ion collisions



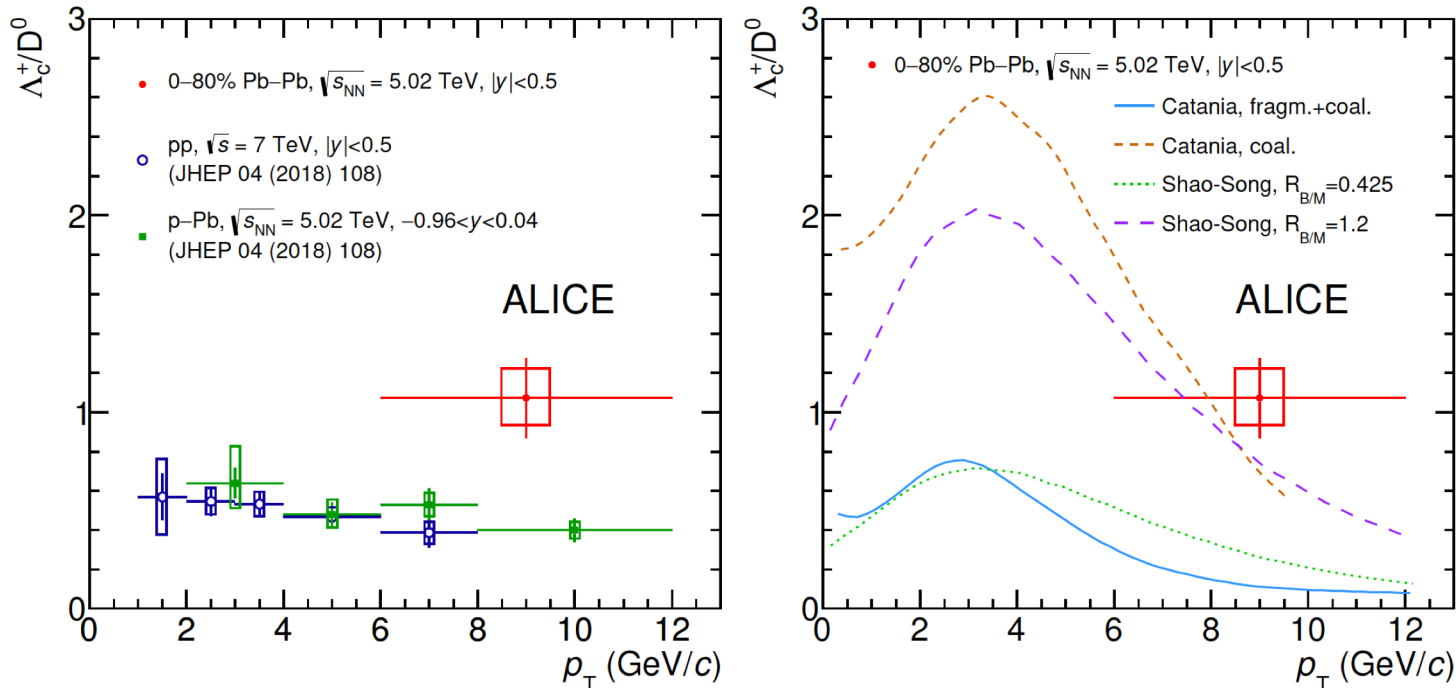
Nucl. Phys. Vol 1005 (2021)121781



- 对比pp和Pb-Pb碰撞中强子（和奇特强子）的产率，可以得到强子尺寸和结合致密度的信息
- 较大尺寸（弱束缚）的强子会被夸克物质分解

Diquarks in QGP?

Phys. Lett. B 793 (2019) 212



- In QGP, two light quarks (e.g. $[ud]$) may form colored bounded state – diquarks.
- In diquark models, a baryon such as Λ_c^+ can be viewed as $c+[ud]$. There will be plenty of diquarks in QGP, so production ratio Λ_c^+/D^0 will be enhanced in A-A compared with p-A and p-p

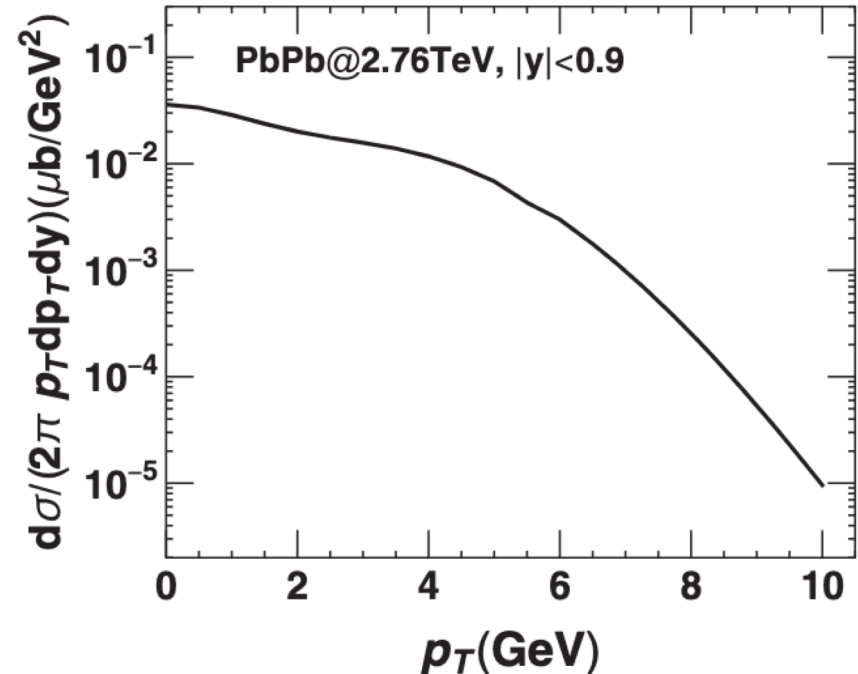
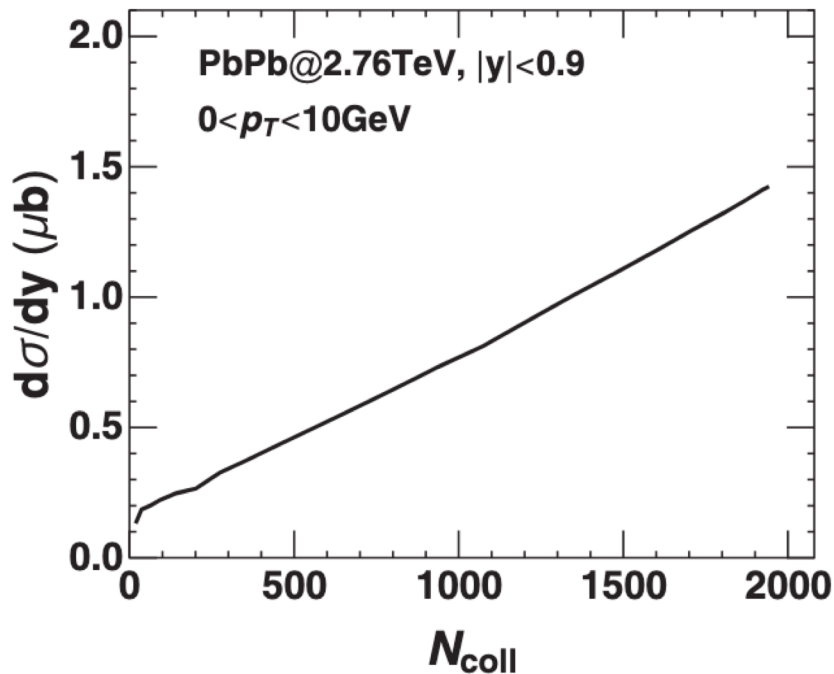
4mu resonance in QGP

[Phys. Rev. D 102 (2020) 114001]

- In QGP, there are different behaviors of $cc\bar{c}\bar{c}$ and $bb\bar{b}\bar{b}$ tetraquark (TQ) states:
 - At critical temperature, $cc\bar{c}\bar{c}$ is already melted due to color screening, while $bb\bar{b}\bar{b}$ TQ state survive in almost all the QGP phase
- In p-p collisions, the main production channel is SPS. In HI collisions, the main production of $cc\bar{c}\bar{c}$ TQ state is by the coalescence mechanism. As a result, the cross section of $cc\bar{c}\bar{c}$ TQ in HI is much larger compared to p-p:
 - Due to the large number of binary collisions in A-A
 - Due to the coalescence mechanism
- If coalescence is main mechanism for $cc\bar{c}\bar{c}$ TQ , then the TQ momentum will be very soft
 - Efficient selection for low p_T muon is crucial for the 4mu analysis in HI data

The $cc\bar{c}\bar{c}$ TQ cross section

[Phys. Rev. D 102 (2020) 114001]



- Left: $cc\bar{c}\bar{c}$ TQ cross section per unit rapidity as a function of the number of binary collisions in Pb-Pb collisions
- Right: transverse momentum distribution of the $cc\bar{c}\bar{c}$ TQ in Pb-Pb collisions

However, the decay BR of $cc\bar{c}\bar{c}$ TQ in a hot medium needs theoretical predictions

Summery

- LHC is the collider at the highest energy frontier in the world. It is a powerful tool to test the SM in both electroweak and QCD sectors, and to look for New Physics including Higgs properties
- The Higgs looks very much like the SM Higgs so far. We need more data to measure its properties more precisely, including next generation collider experiments
- QCD and hadron physics at low energy is hard to make predictions due to the failing of perturbativity. Study of exotic hadrons made up four or five quarks deepens our understanding in this regime
- QCD and hadron physics can be better studied by comparing the p-p and A-A collision events. The effect novel matter of QGP can show up in the comparisons